HELLENIC REPUBLIC
National and Kapodistrian University of Athens
EST. 1837

"ALEXANDER FLEMING"
Biomedical Science Research Centre

Chromatin Profiling Optimization and Drug Response Analysis in Lung Cancer Cell Lines

Christos Christogeorgos

International MSc Molecular Biomedicine

Supervised by: Apostolos Klinakis, Researcher A

Athens 2024

Prologue

In the halls of the Biomedical Research Foundation of the Academy of Athens (BRFAA), where the sound of equipment hums and researchers scurry about, a journey began, a journey fueled by curiosity, collaboration, and guidance.

Under the supervision of Apostolos Klinakis, this dissertation thesis found its footing. His expertise and encouragement provided a steady hand through the complexities of research.

But it wasn't a solo expedition. Dimitris Karagiannis played a pivotal role, offering guidance and friendship in equal measure. Together, we navigated the challenges and celebrated the victories of scientific inquiry.

In the lab, amidst the controlled chaos of experiments, a warm atmosphere prevailed. It was a place where questions were welcomed, and collaboration thrived.

As these pages unfold, they tell the story of teamwork, resilience, and the vibrant community within BRFAA, a community dedicated to advancing knowledge and pushing the boundaries of scientific understanding.

Table of contents

A. Introduction

A.1 Chromatin

The complexes between eukaryotic DNA and proteins are called chromatin, which typically contains about twice as much protein as DNA. The major proteins of chromatin are named histones. They are small proteins containing a high proportion of basic amino acids (arginine and lysine) that facilitate binding to the negatively charged DNA molecule. There are five major types of histones, called H1, H2A, H2B, H3, and H4, which are very similar among different species of eukaryotes. Histones are abundant in eukaryotic cells with their combined mass nearly equaling that of the cell's DNA. Chromatin also includes a diverse array of nonhistone chromosomal proteins, involved in various activities such as DNA replication and gene expression.

Histones are absent in eubacteria like E. coli, although these bacteria associate their DNA with other proteins mimicking histones. On the other hand, archaebacteria do contain histones, packaging their DNA in structures akin to eukaryotic chromatin.

The nucleosome, described by Roger Kornberg in 1974, serves as the basic structural unit of chromatin (Figure 1). Kornberg's nucleosome model emerged from experiments using micrococcal nuclease, revealing 200-base-pair DNA fragments protected by histone binding. Electron microscopy further confirmed the beaded appearance of chromatin fibers, with these beads, or nucleosomes, spaced at approximately 200 base pairs intervals. This model provides a captivating insight into how DNA is organized and protected within the cell.

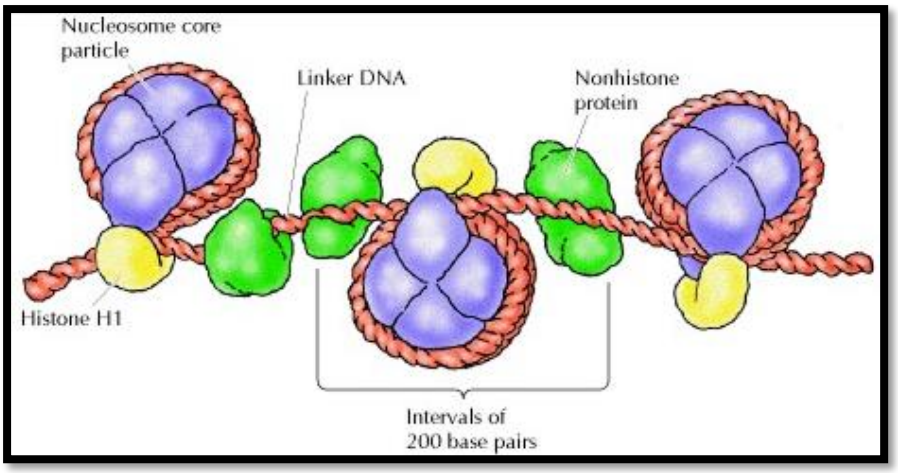

Figure 1. The organization of chromatin in nucleosomes. The DNA is wrapped around histones in nucleosome core particles and sealed by histone H1. Nonhistone proteins bind to the linker DNA between nucleosome core particles. Figure by The Cell: A Molecular Approach. 2nd edition. Cooper GM. Sunderland (MA): Sinauer Associates; 2000.

Throughout the cell's life cycle, the level of chromatin condensation undergoes variations. In non-dividing cells during interphase, the majority of chromatin, termed euchromatin, is in a relatively relaxed state, dispersed throughout the nucleus. During this phase, genes undergo transcription, and DNA replication occurs in preparation for cell division. The euchromatin observed in interphase nuclei is mainly in the form of 30-nm fibers, organized into large loops containing approximately 50 to 100 kb of DNA (Figure 2). Around 10% of euchromatin, which encompasses actively transcribed genes, takes on a more open and decondensed state referred to as the 10-nm conformation, facilitating the transcription process. This intricate interplay between chromatin structure and the regulation of gene expression is a pivotal aspect of eukaryotic cellular dynamics.

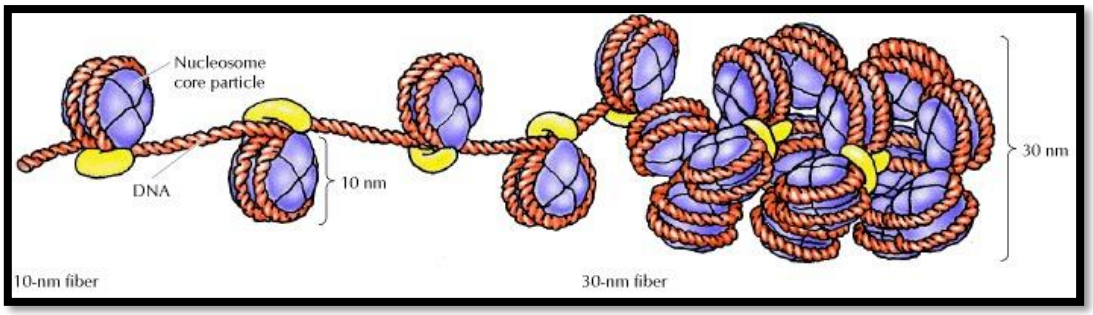

Figure 2. Chromatin fibers. The packaging of DNA into nucleosomes yields a chromatin fiber approximately 10 nm in diameter. The chromatin is further condensed by coiling into a 30-nm fiber, containing about six nucleosomes per turn. Photographs courtesy of Ada L. Olins and Donald E. Olins, Oak Ridge National Laboratory.

In contrast to euchromatin, about 10% of interphase chromatin is in a very highly condensed state that resembles the chromatin of cells undergoing mitosis and it is called heterochromatin. Heterochromatin is transcriptionally inactive and contains highly repeated DNA sequences, such as those present at centromeres and telomeres.

As cells transition into mitosis, their chromosomes go through substantial condensation to enable efficient distribution to daughter cells. The loops created by 30-nm chromatin fibers are believed to undergo additional folding, resulting in the formation of tightly compacted metaphase chromosomes in mitotic cells. This condensation leads to a drastic 10.000-fold reduction in the DNA volume. However, the extensively condensed chromatin in mitosis is no longer suitable for RNA synthesis, resulting in the halting of transcription during this phase. (Chromosomes and Chromatin - The Cell - NCBI Bookshelf, n.d.)

A.2 Regulation of transcription

Transcriptional regulation is a fundamental biological process enabling cells and organisms to respond to internal and external signals, determine cell identity during development, maintain it over time, and coordinate cellular activities. This dynamic mechanism involves numerous molecules orchestrating biophysical events, forming intricate networks, and progressing through multiple temporal and functional stages. These stages encompass specific DNA-protein interactions, recruitment, and assembly of nucleoprotein complexes (Casamassimi & Ciccodicola, 2019).

At its essence, transcriptional regulation involves several key steps: recruitment and assembly of the transcription machinery, initiation, pause release, elongation, and termination of transcription. These steps are intricately connected to chromatin accessibility, modulated by processes like histone modification and chromatin remodeling, as well as other epigenetic mechanisms like enhancer-promoter looping, crucial for successful gene transcription. Additionally, RNA maturation processes such as splicing contribute to the complexity.

A diverse array of molecules and molecular factors participate in transcriptional regulation, including transcription factors, coactivators, corepressors, and chromatin regulators (Lee & Young, 2013). The basal transcription machinery consists of the RNA polymerase II holoenzyme, general initiation transcription factors (TFIIA, -IIB, -IID, -IIE, -IIF, and -IIH), and the Mediator complex. The Mediator complex plays a pivotal role in bridging transcription factors bound at upstream regulatory elements, such as nuclear receptors, with the remaining transcription apparatus at the promoter

region. It also collaborates closely with factors involved in epigenetic modifications, facilitating processes like DNA looping alongside cohesin (Schiano et al., 2014).

Moreover, the intricate nature of transcriptional regulation stems from the involvement of non-coding RNAs (ncRNAs). Over the past two decades, research has unveiled novel classes of ncRNAs, including microRNAs (miRNAs), small nucleolar RNAs (snoRNAs), long ncRNAs (lncRNAs), circular RNAs (circRNAs), and enhancer RNAs (eRNAs). Each of these ncRNAs serves specific regulatory roles, collectively contributing to a broader RNA communication network that ultimately governs protein production. (Casamassimi et al., 2017)

It's common knowledge that a variety of human disorders are marked by broad transcriptional dysregulation, as most signaling pathways ultimately impact the transcription machinery. In fact, numerous syndromes, genetic conditions, and complex diseases, including cancer, autoimmune diseases, neurological and developmental disorders, as well as metabolic and cardiovascular conditions, can result from mutations or changes in regulatory sequences, transcription factors, cofactors, chromatin regulators, non-coding RNAs, and other elements of the transcription apparatus (Casamassimi & Ciccodicola, 2019).

A.3 Histone marks

The fundamental unit of chromatin is the nucleosome, composed of a histone octamer containing two copies each of H3, H4, H2A, and H2B, around which 146 base pairs of DNA are wound. The unstructured N-terminal histone tails extend outward from the nucleosome and undergo various post-translational modifications, known as

histone marks (Gates et al., 2017). The concept of histone marks' potential functional significance was initially proposed by Allfrey in 1964 (Allfrey et al., 1964) and further elaborated into the histone code hypothesis (Strahl & Allis, 2000). Histone marks are regulated by a balance of enzymatic activities, with their precise functions still not fully elucidated. In metazoans, histone protein genes are clustered together (Sierra et al., 1982), complicating direct experimentation on specific histone modification sites in cells or *in vivo*. Consequently, most investigations rely on cell-free systems or manipulate the expression or activity of enzymes involved in histone modification to infer their functions. The enzymes responsible for adding histone marks, known as 'writers,' utilize various cofactors such as ATP, acetyl-CoA, or S-adenosylmethionine (SAM) to catalyze phosphorylation, acetylation, and methylation, respectively. Conversely, 'erasers' enzymes remove histone modifications, while 'readers' proteins directly bind to modified histones, often as components of larger protein complexes that regulate downstream functions through additional enzymes and scaffolds (Gates et al., 2017).

Epigenetic reader proteins contain specific domains that interact with modified histone residues (Musselman et al., 2012). Notably, many reader proteins possess not just one, but often multiple reader domains, suggesting their ability to recognize combinations of various histone marks concurrently. Consequently, the presence or absence of adjacent marks may influence the binding affinity of a reader domain to a specific residue. Among histone proteins, lysine residues are notably abundant (Tan et al., 2011) and more prone to modification compared to other residues. These lysine residues undergo diverse modifications, with methylated and acetylated lysines being the most extensively studied. Specific lysine residues on histone proteins are marked within distinct genomic regions, correlating with different transcriptional states, a

pattern conserved across species. Techniques like Chromatin Immunoprecipitation assays coupled with microarrays (ChIP-chip) and sequencing (ChIP-seq) have provided comprehensive insights into various histone modifications and their genomic locations (Heintzman et al., 2007). Promoters of actively transcribed genes typically exhibit trimethylation on histone H3 lysine 4 (H3K4me3) and acetylation on histones H3 and H4, while actively transcribing genes often display elevated levels of H3K36me3 and H3K79me3 within their gene bodies. Cis-regulatory enhancer elements associated with active transcription are characterized by both H3K27ac and high levels of H3K4me1 relative to H3K4me3 (Figure 3). Conversely, repressed genes tend to have denser nucleosome packing and may bear marks like H3K9 methylation, H3K27me3, and H4K20me3 (Gates et al., 2017).

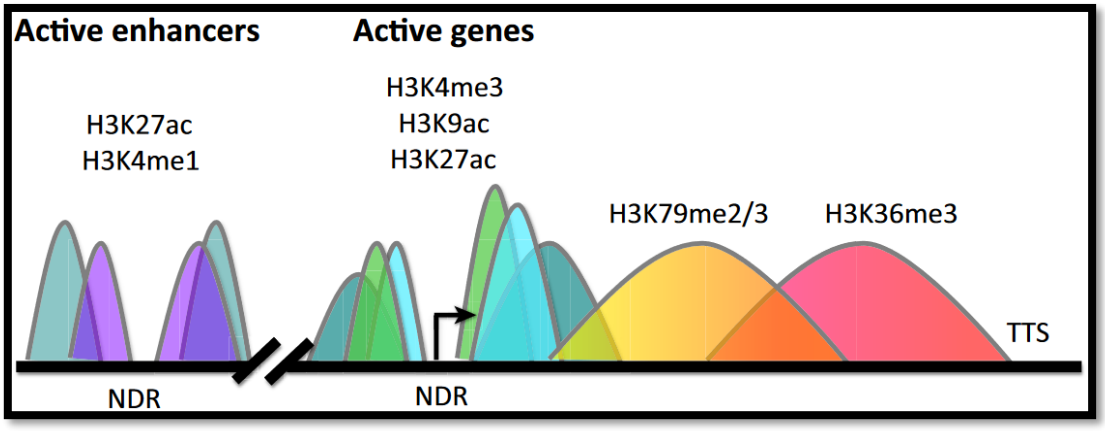

Figure 3. Genomic Localization of Histone H3 Modifications Associated with Active Transcription. Simplified illustration of histone modification occupancy as defined by chromatin immunoprecipitation and sequencing (ChIP-seq) assays is presented. Regions in color represent what a typical ChIP signal would look like at a given eukaryotic gene [teal, acetylation on H3 lysine 27 (H3K27ac); purple, monomethylation on H3 lysine 4 (H3K4me1); light blue, acetylation on H3 lysine 9 (H3K9ac); green, trimethylation on H3 lysine 4 (H3K4me3); yellow/orange, di- and trimethylation on H3 lysine 79 (H3K79me2/3); pink/red, trimethylation on H3 lysine 36 (H3K36me3)]. H3K4me3 and H3K9ac are associated with transcriptionally active gene promoter regions, while H3K36me3 and

H3K79me3 are localized to gene bodies of actively transcribing genes. H3K27ac localizes to both active gene promoters and enhancer regions, and H3K4me1 is predominantly enriched at enhancers. By contrast, repressed genes have different methylation marks and lack histone acetylation (not shown). Arrow denotes the transcription start site (TSS). Abbreviations: NDR, nucleosome-depleted region; TTS, transcription termination site. Figure by: Gates et al., 2017.

A.4 Chromatin regulation enzymes mutated in cancer

In recent years, there has been a growing fascination with how epigenetics influences tumor biology. Epigenetic changes can influence the expression of genes in tumors without directly altering the DNA sequence. These changes, including DNA methylation, modifications to histones, and alterations in nucleosome composition, are pivotal in tumor development and progression. They can be influenced by environmental factors and conditions within the tumor microenvironment. As our understanding of epigenetic processes in cancer has evolved, attention has turned back to the DNA of the tumor itself. Certain genes responsible for regulating chromatin structure and DNA modifications, known as chromatin regulatory factors (CRFs), as well as genes encoding histone proteins, frequently carry mutations in human cancers. These mutations disrupt tumor chromatin and DNA structure, ultimately leading to changes in the epigenetic landscape and gene expression patterns that contribute to cancer development. These mutated CRFs have now been identified across various cancer types and are increasingly considered as promising targets for cancer therapies (Koschmann et al., 2017).

It's not surprising that proteins so integral to gene expression patterns can profoundly disrupt cellular behavior when mutated. Changes in genes encoding chromatin regulatory factors (CRFs), such as point mutations, amplifications, deletions, and fusions, can trap cancer cells in an abnormal epigenetic state, fostering continuous self-renewal without differentiation (Shen & Laird, 2013). Some mutations in CRFs act as driver mutations of many human malignancies, sometimes being the sole driving force behind tumor growth. Furthermore, mutations in enzymes that produce metabolites utilized by CRFs can also fuel cancer development. For instance, various human cancers exhibit gain-of-function point mutations in isocitrate dehydrogenase 1 (IDH1), leading to the production of the metabolite 2-hydroxyglutarate instead of α-ketoglutarate. This inhibits α-ketoglutarate-dependent demethylases, resulting in increased methylation of H3K9 and H3K27, hypermethylation of DNA, and suppression of tumor cell differentiation (Lu et al., 2012). Additionally, recurrent gain-of-function point mutations in histone variants HIST1H3A (H3.1) and H3F3A (H3.3) cause significant downstream epigenetic changes, contributing to tumor growth in pediatric glioblastoma, chondroblastoma, and undifferentiated sarcoma (Schwartzentruber et al., 2012).

A.5 DNA damage response

Genomic damage can occur as a side effect of DNA metabolic processes, including replication errors, uncontrolled recombination, off-target mutations induced by somatic hypermutation during antigen production, and inaccurate VDJ recombination (Liu & Schatz, 2009). However, the most significant genomic burden arises from

processes that directly damage DNA. These DNA lesions come from three primary sources (Lindahl, 1993): environmental agents such as ultraviolet light, ionizing radiation, and various genotoxic chemicals; reactive oxygen species (ROS) produced by respiration and lipid peroxidation; and the spontaneous hydrolysis of nucleotide residues, leading to abasic sites and deamination of C, A, G, or 5methyl-C. It is estimated that each cell faces approximately 10.000 to 100.000 lesions daily, highlighting the challenging task of clearing genomic injuries to maintain proper genome function. Critical genome processes, including transcription and replication, are significantly disrupted by DNA lesions. When replication occurs over damaged DNA, it can lead to mutations that may initiate and promote carcinogenesis. Acute effects emerge when lesions obstruct transcription, leading to cellular senescence or apoptosis, which can result in damage-induced accelerated aging (Akbari & Krokan, 2008; Mitchell et al., 2003; Sinclair & Oberdoerffer, 2009). Cells have developed numerous pathways to recognize and repair DNA damage while coordinating a cellular response to minimize the impact of genomic lesions and support effective repair.

A.5.1 Base Excision Repair (BER)

Bases with minor chemical modifications that do not significantly disrupt the DNA double-helix structure are substrates for Base Excision Repair (BER) (Almeida & Sobol, 2007; Hegde et al., 2008). These lesions are targeted by lesion-specific DNA glycosylases, which recognize and remove the damaged base from the sugar-phosphate backbone. The resulting abasic (AP) site is then incised by AP-

endonucleases, and the resulting single nucleotide gap is filled by the BER-specific DNA polymerase β and sealed by the XRCC1/Ligase III complex. Single-strand breaks (SSBs) are repaired by a specialized BER mechanism known as single-strand break repair (SSBR). The abundant nuclear protein Poly-ADP-Ribose-Polymerase (PARP) is rapidly activated by SSBs, leading to auto-poly-ADP-ribosylation. This process recruits the XRCC1/Ligase III complex and end-processing enzymes such as aprataxin (Gueven et al., 2004) and TDP1 (tyrosyl-DNA-phosphodiesterase) to create ligatable DNA ends (Caldecott, 2007; El-Khamisy et al., 2009).

A.5.2 Nucleotide Excision Repair (NER)

Nucleotide Excision Repair (NER) removes a wide range of single-strand lesions that cause local helix destabilization. NER is a complex, multi-step process involving the coordinated action of at least 25 different polypeptides (Gillet & Schärer, 2006; Hoeijmakers, 1993). There are two distinct modes of damage detection in NER: transcription-coupled NER (TC-NER) and global genome NER (GG-NER). TC-NER efficiently removes lesions that stall transcription, allowing transcription to resume quickly (Bohr et al., 1986; Hanawalt, 1994), while GG-NER detects lesions throughout the genome.

In TC-NER, the stalled RNA polymerase senses the damage, and the Cockayne syndrome factors A and B (CSA and CSB) are crucial for assembling the TC-NER complex (Fousteri et al., 2006; Fousteri & Mullenders, 2008). In GG-NER, lesion recognition is carried out by the XPC/hHR23B (Masutani et al., 1994) and UV-DDB

(DDB1 and DDB2/XPE) complexes (Chu & Chang, 1988; Keeney et al., 1994; Sugasawa et al., 2009).

The subsequent steps of TC-NER and GG-NER converge into a common pathway where the NER/basal transcription factor TFIIH is first recruited (Volker et al., 2001; Yokoi et al., 2000). The bi-directional helicase activity of TFIIH unwinds the damaged DNA segment over approximately 30 nucleotides (Sugasawa et al., 2009). The unwound DNA is stabilized by XPA and RPA (Replication Protein A), which also help position the two structure-specific endonucleases, XPG and the ERCC1-XPF complex (Figure 4). These endonucleases make incisions on the damaged strand 3′ and 5′ to the lesion, respectively (O'Donovan et al., 1994; Sijbers et al., 1996).

The resulting 25–30 nucleotide single-strand gap is then filled in by standard DNA replication proteins, including replication factor C (RFC), PCNA, RPA, and DNA polymerases δ, ε, or κ (Ogi et al., 2010). Finally, the gap is sealed by DNA ligases I or III, depending on the cell's proliferation status (Moser et al., 2007).

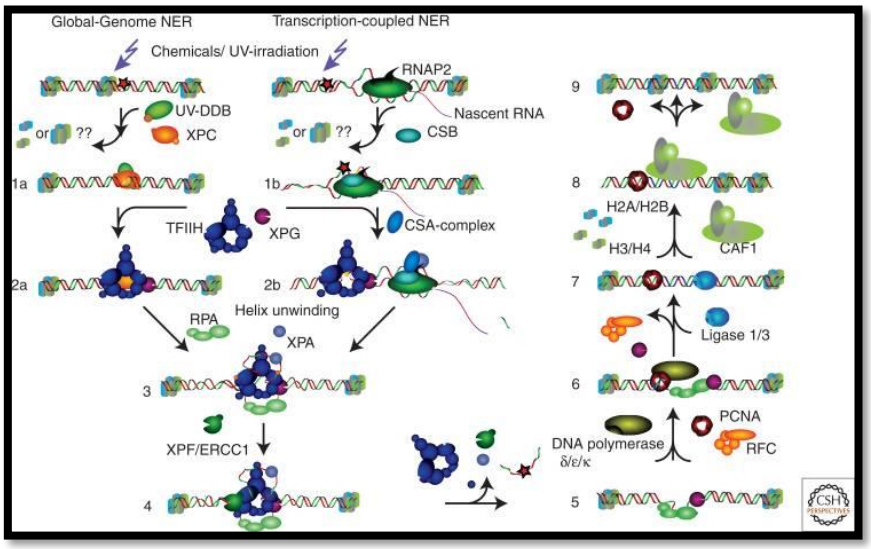

Figure 4. Molecular mechanism of nucleotide excision repair (NER). Figure by Giglia-Mari et al., 2011.

A.5.3 DNA Double-Strand Break (DSB) Repair

Lesions that are substrates for NER and BER are located on one of the DNA strands and are removed through a "cut-and-patch" mechanism. In both processes, the undamaged complementary strand serves as a template for repairing the damaged strand. However, some damaging agents affect both strands, such as ionizing radiation, which induces DNA double-strand breaks (DSBs), and agents that produce inter- and intra-strand cross-links. These lesions are highly cytotoxic because they are more challenging to repair, as the cell cannot simply copy information from an undamaged strand (Giglia-Mari et al., 2011).

Two distinct pathways repair the majority of DSBs: homologous recombination (HR) and non-homologous end-joining (NHEJ) (Cahill et al., 2006; Helleday et al., 2007; Wyman & Kanaar, 2006). The choice between these repair mechanisms is primarily determined by the cell cycle phase. HR, which requires a homologous sister chromatid, operates exclusively in the S and G2 phases. In contrast, post-mitotic cells and cycling cells in the G1 phase must repair DSBs using NHEJ.

In NHEJ, breaks are quickly recognized by the Ku70/Ku80 heterodimer, which activates the PI3-kinase DNA-PK and facilitates the recruitment of the Artemis nuclease and the MRE11/Rad50/NBS1 (MRN) protein complex. These proteins are involved in DNA end-processing, which precedes ligation by the XRCC4/Ligase IV complex (Burma et al., 2006; Van Gent & Van Der Burg, 2007; Weterings & Van Gent, 2004). During this end-processing, minor nucleotide losses or changes may occur, making NHEJ an error-prone repair process despite its rapid action.

When cells have a homologous template available, such as during the S and G2 phases, DSBs can be repaired by HR. Homologous recombination begins with the binding of the MRN complex to a DSB, which helps hold the broken ends together (De Jager et al., 2001) and provides the structural basis for the CtIP nuclease. The MRN-CtIP complex, along with exonuclease I (EXO1), catalyzes end resection at the break (Limbo et al., 2007; Sartori et al., 2007; Takeda et al., 2007). RPA then binds to the newly formed single-strand region, and through a complex handoff mechanism, the RPA filament is replaced by a RAD51 nucleoprotein filament. This RAD51 filament is essential for strand invasion into the homologous sister chromatid, creating a temporary triplex DNA structure where strand exchange occurs (Wyman et al., 2004). Alternative pathways for repairing double-strand breaks (DSBs), such as alternative end-joining (a-EJ) and single-strand annealing (SSA), are error-prone mechanisms used when primary repair pathways fail. a-EJ relies on microhomologies to align DNA ends, often causing small insertions or deletions, while SSA uses longer homologous sequences, leading to large deletions (Caracciolo et al., 2021). Both pathways contribute to genomic instability and are associated with tumorigenesis, particularly in HR-deficient cells.

A.5.4 BRCA genes

Individuals who carry harmful heterozygous germline mutations in the *BRCA1* and *BRCA2* genes face a significantly higher risk of developing breast, ovarian, and other types of cancer (King, 2014; Miki et al., 1994; Wooster et al., 1995). These genes are classified as classical tumor suppressors because the loss of the normal *BRCA1* and

BRCA2 alleles occurs during tumor development (Lord & Ashworth, 2017). The BRCA1 and BRCA2 proteins play a crucial role in repairing double-strand DNA breaks through a process called homologous recombination repair (HRR), a DNA repair mechanism that uses a homologous DNA sequence to accurately restore the original DNA at the site of damage (Moynahan & Jasin, 2010). When cells lose HRR functionality due to defects in BRCA1, BRCA2, or other related components, non-conservative DNA repair mechanisms, such as Non-Homologous End Joining (NHEJ), become dominant. These alternative processes either join broken DNA ends without using a homologous sequence or fuse nearby DNA regions with short sequence homology, often leading to the deletion of intervening genetic material. The increased reliance on these error-prone repair mechanisms in the absence of HRR often results in DNA alterations, including deletions, which can contribute to cancer initiation or progression (Moynahan et al., 2001; Tutt et al., 2001). This may help explain why mutations in *BRCA1* and *BRCA2* elevate cancer risk. Additionally, the roles of BRCA1 and BRCA2 in chromatin remodeling and transcriptional regulation could also be relevant to the development of cancer (Dhillon et al., 2016).

A.5.5 Poly(ADP-Ribose) Polymerases

Healthy cells protect themselves from the harmful effects of DNA damage through a network of interconnected molecular pathways known as the DNA damage response (DDR). These pathways detect DNA damage, halt the cell cycle, and facilitate DNA repair, thereby preserving the integrity of the genome. Central to the DDR are the enzymes Poly(ADP-ribose) Polymerase 1 and 2 (PARP1 and PARP2), which act as

DNA damage sensors and signal transducers. They function by synthesizing negatively charged, branched poly(ADP-ribose) (PAR) chains on target proteins, a post-translational modification process called PARylation (Satoh & Lindahl, 1992). When PARP1 binds to damaged DNA, such as single-strand breaks (SSBs) and other lesions, it undergoes structural changes that activate its catalytic function (Dawicki-McKenna et al., 2015; Satoh & Lindahl, 1992). This activation leads to the PARylation and recruitment of DNA repair proteins like XRCC1, as well as the remodeling of chromatin around the damaged site to facilitate DNA repair. PARP1 eventually undergoes auto-PARylation, where the PAR chains' negative charge likely prompts its release from the repaired DNA (Dawicki-McKenna et al., 2015; Satoh & Lindahl, 1992).

A.5.6 Synthetic Lethality (SL)

In 2005, two research groups reported a Synthetic Lethal (SL) interaction between PARP inhibition and mutations in *BRCA1* or *BRCA2*, proposing a new approach for treating patients with BRCA-mutant tumors (Bryant et al., 2005; Farmer et al., 2005). SL is a concept first introduced by geneticists nearly a century ago to describe a situation where a defect in either of two genes has minimal effect on the cell or organism, but a combination of defects in both leads to cell death (Figure 5). It was shown that BRCA-mutant tumor cells were up to 1000 times more sensitive to PARP inhibitors (PARPi) than BRCA-wild type cells, depending on the specific PARPi and experimental conditions used (Farmer et al., 2005). This finding motivated the testing of PARPi in clinical trials as standalone treatments. The initial hypothesis was that

PARP inhibition caused persistent single-strand breaks (SSBs) which, when encountered by a replication fork, could lead to fork collapse and potentially double-strand breaks (DSBs) (Farmer et al., 2005). However, this model has recently been revised based on evidence suggesting that some PARPi, particularly rucaparib, olaparib, niraparib, and talazoparib, "trap" PARP1 on DNA. This trapping prevents auto-PARylation and the release of PARP1 from the site of damage, thereby disrupting the catalytic cycle of PARP1 (Murai et al., 2012, 2014; Pommier et al., 2016). The trapped PARP1 protein is thought to be the relevant cytotoxic lesion for some PARPi, similar to how certain cancer drugs that inhibit Topoisomerase II trap a DNA repair protein on the double helix. Supporting this idea, cells lacking PARP1 appear to be resistant to PARPi (Murai et al., 2012; Pettitt et al., 2013). Clinically used PARPi vary in their ability to trap PARP1. For instance, talazoparib is approximately 100 times more potent than niraparib in this regard, and niraparib is more potent than olaparib and rucaparib (Murai et al., 2014).

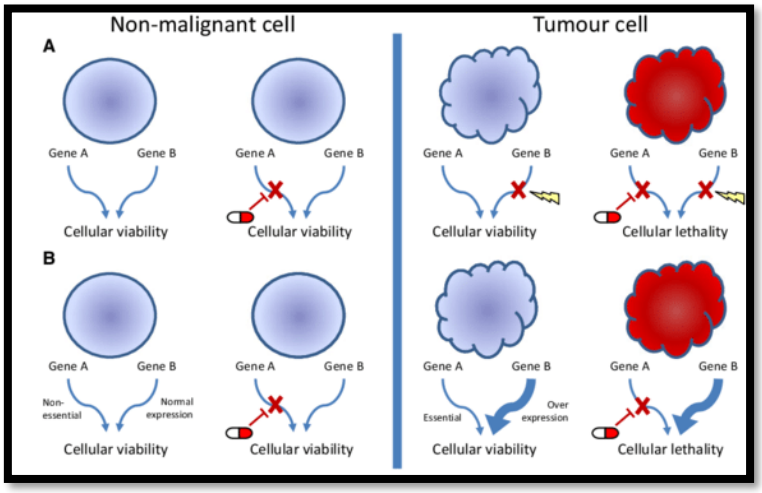

Figure 5. The concept of using synthetic lethality as a therapeutic strategy in cancer. (A) Synthetic lethality: The loss of gene A or gene B in isolation is compatible with cellular viability, whereas loss of both genes together leads to cellular lethality. (B) Synthetic dose lethality: Overexpression or overactivation of gene B leads to cellular dependence on gene A. Figure by Thompson et al., 2017.

A.6 Non-Small Cell Lung Cancer

Lung cancer ranks as the primary cause of cancer-related deaths in both men and women, with non-small cell lung cancer (NSCLC) constituting approximately 85% of all lung cancer cases. Typically, at the time of diagnosis, the tumor has progressed to a locally advanced or metastatic stage, leading to unfavorable disease outcomes. NSCLC encompasses adenocarcinoma, squamous cell carcinoma, and large cell lung carcinoma. There is a pressing need to identify new therapeutic targets due to the limited efficacy of platinum-based therapy and the targeted therapies developed over the past decade. The latter is primarily attributed to the absence of detectable mutations in approximately half of all NSCLC cases. Additionally, there is a necessity for novel therapeutic approaches to enhance the effectiveness of immunotherapy in NSCLC. The identification of molecular signatures within NSCLC subtypes, including genetic and epigenetic variations, is essential for the selection of appropriate therapy or combinations of therapies. Epigenetic dysregulation plays a pivotal role in tumor development, heterogeneity, and resistance to conventional anti-cancer treatments. Consequently, epigenomic modulation has emerged as a promising therapeutic strategy in NSCLC (Bajbouj et al., 2021).

A.6.1 DNA methylation in lung cancer

DNA methylation is the most studied epigenetic regulatory mechanism. CpG island methylation is completed by different DNA methyltransferases (DNMTs) that can lead to gene silencing. Three active DNMTs (DNMT1, DNMT3a, and DNMT3b)

mediate the transfer of a methyl group from S-adenosyl-L-methionine to the CpG islands 5'-cytosine carbon (Forde et al., 2014). DNMT1 binds essentially to hemimethylated DNA and is primarily involved in the maintenance methylation after DNA replication. DNMT3a and b bind preferentially to unmethylated or hemimethylated DNA, and are responsible of de novo DNA methylation (Fabbri et al., 2007)

DNMT overexpression plays a significant role in the development of lung cancer. Elevated levels of DNMT in lung cancer can stem from several factors, including increased expression of transcriptional activators, the loss of microRNAs that normally suppress DNMT expression, and/or impaired degradation of DNMT by hsp90 within the proteasome (Damiani et al., 2008). Clinically, there is evidence linking DNMT1 overexpression to poorer survival rates in surgically treated lung cancer patients (Kim et al., 2006). Consistent with these findings, various tumor suppressor genes (TSGs) are silenced through promoter hypermethylation in lung cancer. These TSGs regulate critical cellular functions such as cell cycle progression (p16), DNA repair (MGMT), apoptosis (DAPK, caspase-8), Wnt signaling (APC), cell adhesion, invasion (E-cadherin, H-cadherin, tissue inhibitor of metalloproteinase-3), and invasion suppression (CDH13, TIMP-3). For instance, Brock et al. (Brock et al., 2008) observed that methylation of *CDK2*, *CDKN2A*, *CDH13*, *RASSF1A*, and *APC* correlated with cancer recurrence following surgical resection of stage I non-small cell lung cancer (NSCLC), irrespective of histology, stage, gender, or smoking history. Similarly, another study reported that methylation of *CDKN2A*, accompanied by loss of p16 expression, was associated with reduced survival rates after early-stage NSCLC resection (Sterlacci et al., 2011). Additionally, methylation of *IGFBP-3* is linked to cisplatin resistance in NSCLC (De Caceres et al., 2010).

A.6.2 Histone modifications in lung cancer

Over the past decade, numerous studies have illuminated epigenetic irregularities involving histone modifications in lung cancer. Miyanaga et al. (Miyanaga et al., 2008) examined 16 NSCLC cell lines using HDAC inhibitors such as TSA and vorinostat, both of which exhibited anti-tumor effects in half of the NSCLC cell lines tested. They also conducted gene expression profiling and developed a nine-gene classifier capable of predicting the sensitivity of NSCLC cell lines to HDAC inhibitor drugs (Miyanaga et al., 2008). Van Den Broeck et al. (Van Den Broeck et al., 2008a) demonstrated the pivotal role of histone epigenetic modifications in lung carcinogenesis. Lung cancer cells exhibited aberrant patterns of histone H4 modification compared to normal lung cells, characterized by hyperacetylation of H4K5/H4K8, hypoacetylation of H4K12/H4K16, and loss of H4K20 trimethylation. These findings underscore the significance of histone H4 modifications and suggest H4K20me3 as a potential biomarker for early detection and therapeutic strategies in lung cancer (Van Den Broeck et al., 2008a). Seligson et al. (Seligson et al., 2009) showed that decreased global levels of histone modifications predict a more aggressive cancer phenotype in lung AdC. Moreover, the distinct expression patterns of HATs and HDACs in tumor samples, compared to normal tissues, may have therapeutic implications, including early tumor detection, prognosis assessment, and guiding epigenetic-targeted therapies (Özdağ et al., 2006). *HDAC1* gene expression appears to correlate with the progression of lung cancer, with elevated *HDAC1* and *HDAC3* gene expressions associated with poor prognosis in patients with pulmonary AdC (Sasaki et al., 2004). HDAC3 was also found to be elevated in 92% of tumors with SqCC histology using antibody microarrays for protein detection (Bartling et al.,

2005). NSCLC cells treated with HDIs showed decreased TNF-receptor-1 mRNA and protein levels, as well as reduced surface protein expression, resulting in attenuated NF-B nuclear translocation and DNA binding in response to TNF treatment. Thus, HDIs may offer beneficial contributions to tumor treatment by reducing tumor cell responsiveness to TNF-mediated activation of the NF-B pathway (Imre et al., 2006).

A.6.3 Epigenetic biomarkers in lung cancer

Recent research has intensively investigated epigenetic alterations as potential biomarkers for early detection, diagnosis, prognosis, and guiding therapeutic strategies in lung cancer. This research has predominantly concentrated on DNA cytosine methylation, miRNA alterations, and histone modifications (Balgkouranidou et al., 2013a; Brzeziańska et al., 2013a; Jones & Baylin, 2002a; Van Den Broeck et al., 2008b). Each of these epigenetic changes requires specific testing methods and varies in its clinical relevance. Currently, most epigenetic biomarkers for lung cancer are still in the developmental stage and are unlikely to be clinically applicable for several years (Liloglou et al., 2014).

A.6.4 DNA hypermethylation

DNA 5'-cytosine hypermethylation emerges as an early event in the development of lung cancer (Balgkouranidou et al., 2013b; Brzeziańska et al., 2013b; Jones & Baylin, 2002b). Numerous genes undergo hypermethylation in lung cancer, including *PAK3*,

NISCH, *KIF1A*, *OGDHL*, *BRMS1*, *FHIT*, *CTSZ*, *CCNA1*, *NRCAM*, *LOX*, *MGMT*, *DOK1*, *SOX15*, *TCF21*, *DAPK*, *RAR*, *RASSF1*, *CYGB*, *MSX1*, *BNC1*, *CTSZ*, and *CDKN2A* (Shames et al., 2006a; Wang et al., 2007). The extent of hypermethylation varies for each gene, with some, like *CDKN2A* and *MGMT*, exhibiting hypermethylation in 100% of pulmonary SqCC patients up to 3 years before cancer diagnosis (Weinberg, 1995). Functionally, p16 acts to inhibit cyclin-dependent kinases 4 and 6, which, upon binding to cyclin D1, phosphorylate and deactivate the retinoblastoma tumor suppressor gene, thereby halting cell cycle progression (Weinberg, 1995). In approximately 70% of lung cancer cases, p16 loss occurs, often through promoter methylation, facilitating the transition from G1 to S phase (Shackelford et al., 1999; Weinberg, 1995). Notably, *CDKN2A* methylation is observed in seemingly normal epithelium from smokers and precursor lesions, with its frequency increasing with the advancement of the carcinogenic process (Belinsky et al., 1998). The precise mechanisms underlying each gene's hypermethylation event in promoting cancer vary, but generally involve the suppression of tumor suppressor genes alongside the activation of genes promoting cell growth and cycle progression (Shames et al., 2006b; Toyota et al., 1999a).

Numerous studies have consistently shown that changes in cytosine hypermethylation hold diagnostic (J. Li et al., 2017; Ozsolak et al., 2008a; Shames et al., 2006c; Toyota et al., 1999b) and prognostic significance in lung cancer, and in certain instances, they may even forecast responses to treatment (Cross et al., 1994; Ehrich et al., 2005; Goll & Bestor, 2005; Korch & Hagblom, 1986; Rauch & Pfeifer, 2005; Zhang et al., 2011). For instance, Zhang et al. (Y. Zhang et al., 2011) investigated the methylation patterns of 20 tumor suppressor genes (TSGs) in 78 cases of non-small cell lung cancers (NSCLCs) in comparison to 50 plasma samples from cancer-free individuals. They

identified a set of five genes (*APC*, *RASSF1A*, *CHD13*, *KLK10*, and *DLEC1*) exhibiting significantly higher methylation levels in lung cancer patients, with a sensitivity of 83.64% and specificity of 74.0% for cancer diagnosis within the Chinese population. Additionally, in a subset of 64 lung cancer patients, those with four or more concurrently methylated genes from a panel of 15 genes had a poorer progression-free two-year survival (13.8 months) compared to those with fewer methylated genes (17.8 months). Furthermore, a study conducted by Salazar et al. (Salazar et al., 2011) revealed that lung cancer patients with an unmethylated plasma *CHFR* gene showed significantly better responses to EGFR tyrosine kinase inhibitors than those with a methylated *CHFR* gene. This finding underscores the potential utility of gene methylation patterns in predicting responses to therapy.

A.6.5 MicroRNA and microRNA silencing in lung cancer

MicroRNAs (miRs) are short, naturally occurring RNA molecules, typically consisting of 20–22 nucleotides, that play a crucial role in regulating gene expression. With over 1000 miRs identified so far, they govern the activity of more than one-third of protein-coding messenger RNAs (mRNAs), with each miR capable of controlling the expression of hundreds of target mRNAs (He & Hannon, 2004). Consequently, the suppression of miRs through methylation can significantly impact the development and progression of tumors (Ozsolak et al., 2008b). In their research, Heller et al. (Heller et al., 2012) demonstrated that treatment with demethylating agents led to the increased expression of 33 miRs in A549 cells, a type of lung adenocarcinoma (lung AdC). Furthermore, specific miRs such as miR-9-3, miR-34b,

and miR-126 exhibit methylation patterns associated with non-small cell lung cancer (NSCLC) prognosis alteration. Additionally, miR-487b is frequently silenced by methylation in primary lung tumors, and its levels are diminished in respiratory epithelial cells and lung tumor-derived cell lines following exposure to tobacco smoke (Xi et al., 2013). This discovery underscores previous findings indicating the influence of smoking on methylation processes, thereby promoting lung cancer development.

A.6.6 Treatment of early-stage lung cancer

Surgery is recommended for early-stage (I-II) NSCLC, with 5-year survival rates varying by stage. Video-assisted surgery offers better quality of life and outcomes than open surgery, and perioperative chemotherapy provides a survival benefit for stages IB-IIIA. Targeted therapies like EGFR TKIs have shown no significant benefit in unselected patients, but ongoing studies are investigating their role in specific mutations. For stage I patients who can't undergo surgery, stereotactic body radiation therapy (SBRT) is effective. For locally advanced stages (IIIA-B) not suitable for surgery, a combination of chemotherapy and thoracic radiotherapy is the standard treatment, with median survival times over 2 years and 5-year survival rates of 15-20% (Hirsch et al., 2017).

A.6.7 Treatment of advanced lung cancer

Therapeutic advancements in specific subgroups of NSCLC are primarily due to the accumulation of molecular insights gained through emerging technology platforms, such as next-generation sequencing and other omics technologies. These advancements, along with the development of new drugs targeting molecular abnormalities, have greatly benefited patients with tumors that have specific genomic alterations. As many as 69% of patients with advanced NSCLC may have molecular targets that could be addressed by these therapies (Tsao et al., 2016). Progress in molecular targeted therapies has been most notable among younger patients with adenocarcinoma, particularly those who have never smoked. For advanced NSCLC patients who do not qualify for an approved molecular targeted therapy, platinum-based doublet therapy, with or without bevacizumab, remains the standard first-line treatment, though bevacizumab is not suitable for squamous cell histology. Additionally, understanding the immune landscape of tumors and their immune-evasion mechanisms has led to significant therapeutic breakthroughs and established a foundation for future treatment developments (Hirsch et al., 2017).

A.6.8 Immunotherapy

Lung cancer progression is influenced by both the genetic and molecular characteristics of cancer cells and their interaction with the immune system. Traditional immune-based therapies, like vaccines, have largely been ineffective, likely due to inadequate immune activation. Immunotherapy now focuses on

inhibiting or stimulating immune checkpoints, such as PD-1 and PD-L1, which regulate immune responses. Antibodies targeting these checkpoints (e.g., nivolumab, pembrolizumab) have shown promising results, particularly in patients with PD-L1-positive tumors, leading to improved survival rates. However, the variability in PD-L1 testing methods and expression levels complicates predicting which patients will benefit. Current trials are exploring these therapies in different settings and patient groups (Hirsch et al., 2017).

A.6.9 Maintenance therapy for patients with advanced NSCLC

The ideal duration of treatment for patients with advanced NSCLC has been explored in numerous studies. Administering 4-6 cycles of combination chemotherapy followed by observation has become the standard approach for first-line treatment (Ramalingam et al., 2011). To date, strategies involving either switch therapy (using a different treatment than the initial one) with pemetrexed and erlotinib, or continuation maintenance with pemetrexed, have shown improvements in outcomes, including overall survival and progression-free survival. Multiple meta-analyses have confirmed the positive impact of maintenance treatments on both efficacy and toxicity. Overall, these studies have demonstrated that maintenance therapy significantly improves progression-free survival and, to a lesser extent, overall survival, while introducing some clinically relevant toxicities but preserving patients' quality of life. In practice, switch maintenance strategies are less commonly used than continuation maintenance, as both physicians and patients often prefer to maximize the benefit from a given therapy before moving to an alternative. Maintenance therapy with an EGFR inhibitor

is recommended for patients with activating EGFR TKI-sensitizing mutations who, for any reason (such as delayed EGFR mutation profiling), receive first-line chemotherapy (Zhao et al., 2015). Several factors influence the decision to pursue maintenance therapy, including tumor histology (with pemetrexed recommended only for non-squamous NSCLC), genomics, response to induction therapy, patient health status, and, importantly, patient preference. From the patient's perspective, a survival benefit of several months or better symptom control is expected to outweigh mild-to-moderate side effects (Hirsch et al., 2017).

A.6.10 Adjuvant and neoadjuvant systemic therapies

Lung cancer continues to be a leading cause of cancer-related deaths globally. The majority of lung cancers are non-small cell lung cancers (NSCLC), with about one-third of cases being surgically resectable. Over time, there have been gradual improvements in survival rates. However, even after complete tumor removal, up to 60% of patients experience recurrence, often as distant metastases, leading to poor overall survival (OS). This highlights the need for additional therapy beyond surgery. Perioperative systemic therapy aims to target micrometastases to prevent distant spread and can be administered either before surgery (neoadjuvant) or after surgery (adjuvant). Currently, adjuvant chemotherapy is the standard treatment for surgically resected stage IB-IIIA NSCLC. Neoadjuvant chemotherapy, though once considered, showed only modest benefits and was not established as a standard care approach, despite similar OS outcomes between neoadjuvant and adjuvant chemotherapy. Recent advances in understanding cancer biology, particularly the immune system's

role and the development of immune checkpoint inhibitors (ICIs), have renewed interest in neoadjuvant therapy. ICIs have demonstrated durable responses and longer survival in 20%-30% of patients with advanced NSCLC, prompting their consideration in early-stage NSCLC. Studies on neoadjuvant ICIs have shown promising pathological response rates and progression-free survival (John & Ramnath, 2023).

A.7 Modern epigenetics methods in biological research

As the field of epigenetics continues to grow, there's a rising curiosity about exploring new technologies to unravel the epigenetic markers linked to both health and disease. This surge in interest has led to the development of numerous novel techniques within the epigenetics realm. These cutting-edge methods can discern chromatin states across various dimensions, ranging from specific loci analysis to comprehensive genome-wide sequencing. Progress in epigenetics methodologies employs diverse approaches, including the use of top-tier antibodies, chromatin functional assays, imaging techniques, high-throughput sequencing technologies, and integrated bioinformatics pipelines (Y. Li, 2021).

A.7.1 DNA methylation

DNA methylation stands as a pivotal epigenetic mechanism under thorough scrutiny. Within this domain, distinct DNA methylation modifications emerge, including 5-

methylcytosine (5mC), N6-methyladenine (6mA), and 4-methylcytosine (4mC) (Chen et al., 2016; G. Zhang et al., 2015). While 6mA and 4mC predominantly inhabit prokaryotic genomes, 5mC reigns as the most prevalent methylation form across eukaryotes, garnering extensive study and understanding as the foremost DNA modification pattern overall (Jones & Takai, 2001). Various conventional techniques exist for analyzing DNA methylation levels, with bisulfite modification serving as the cornerstone for most assays. This process transforms cytosine to uracil in single-stranded DNA while leaving 5mC unaffected (Frommer et al., 1992). Alternatively, other methods rely on the enzymatic digestion of genomic DNA by specific endonucleases with varying methylation sensitivities to estimate overall DNA methylation levels (Melnikov et al., 2005). These modifications enable the assessment of DNA methylation status at specific loci or on a global scale through multiple techniques. Over recent decades, significant advancements have revolutionized DNA methylation analysis methodologies. For instance, emerging third-generation sequencing-based technologies now facilitate lengthy sequence readings, presenting exciting avenues for studying an array of base modifications, including 5mC, 6mA, and 4mC, without necessitating bisulfite treatment (Schadt et al., 2010). Moreover, techniques capable of identifying oxidized forms of 5mC, such as 5-hydroxymethylcytosine (5hmC), have been developed, further expanding the analytical toolkit in this field (Yu et al., 2012).

A.7.2 Histone modification

Regarding another significant aspect of the epigenetic code, a multitude of technologies has emerged to probe the functions and dynamics of histone modifications. Primarily, these advancements stem from the chromatin immunoprecipitation (ChIP) assay platform (Bannister & Kouzarides, 2011; Gade & Kalvakolanu, 2012). Particularly valuable is the antibody-directed ChIP assay, which enables the examination of DNA-protein interactions, thereby permitting the analysis of chromatin structure surrounding specific DNA sequences. This assay can also be amalgamated with other techniques to delve into the interaction of histone modifications with additional chromatin regulators at specific loci (Davies et al., 2017). Moreover, the three-dimensional (3D) spatial organization of chromatin, which links chromatin structure to biological functionalities, can be deciphered using chromosome conformation capture (3C) technology (Qi & Zhang, 2019). When coupled with ChIP-sequencing and 3C-based methodologies like Hi-C, these approaches facilitate the prediction of epigenetic landscapes within 3D chromatin architecture. Such predictions unveil the interplay between patterns of histone modifications and the 3D spatial disposition of chromosomes, elucidating their roles in regulating biological functions within eukaryotic cells (Di Pierro et al., 2017).

A.7.3 CUT&RUN

Chromatin immunoprecipitation with sequencing (ChIP-seq) and its derivatives encounter challenges such as diminished signals, elevated background noise, and epitope concealment induced by cross-linking, alongside low yields necessitating a substantial quantity of cells (Policastro & Zentner, 2018; Teytelman et al., 2013). Options beyond ChIP involve enzyme-tethering techniques applicable to non-fixed cells, like DamID (Van Steensel et al., 2001), ChEC-seq (Zentner et al., 2015), and CUT&RUN (Skene et al., 2018; Skene & Henikoff, 2017). These methods entail the direct targeting of a particular protein of interest within its cellular context, followed by genome-wide profiling. As an illustration, CUT&RUN, derived from Laemmli's Chromatin ImmunoCleavage (ChIC) strategy (Schmid et al., 2004), delineates chromatin proteins through a series of steps. It involves the sequential binding of a specific antibody followed by anchoring a Protein A/Micrococcal Nuclease (pA-MNase) fusion protein in permeabilized cells, all without cross-linking (Skene & Henikoff, 2017). Activation of MNase with calcium liberates fragments into the supernatant for subsequent DNA extraction, library preparation, and paired-end sequencing. CUT&RUN delivers specific chromatin component resolution at the base-pair level with significantly reduced background levels compared to ChIP-seq, thereby lowering genome-wide profiling costs considerably. Despite its capability to yield high-quality data from as few as 100–1000 cells, CUT&RUN necessitates additional steps such as DNA end polishing and adapter ligation for library preparation, thereby augmenting the time, cost, and effort of the overall procedure. Furthermore, the release of MNase-cleaved fragments into the supernatant in

CUT&RUN renders it unsuitable for integration into single-cell platforms (Mezger et al., 2018; Zheng et al., 2017).

A.7.4 CUT&Tag

Kaya-Okur et al. overcame the limitations of ChIP-seq and CUT&RUN using a transposome that consists of a hyperactive Tn5 transposase (Picelli et al., 2014; Reznikoff, 2003) fused with Protein A (pA-Tn5) and also loaded with sequencing adapters (Kaya-Okur et al., 2019). Through in situ tethering followed by pA-Tn5 activation, factor-targeted tagmentation occurs, producing fragments primed for PCR enrichment and DNA sequencing. With an initial step involving live cells, this method, termed Cleavage Under Targets and Tagmentation (CUT&Tag), yields amplified, sequence-ready libraries within a day, either at the benchtop or in a high-throughput setup. CUT&Tag allows profiling of various chromatin components with remarkably low backgrounds, using minimal cell numbers and even single cells. This straightforward, cost-effective approach promises to revolutionize epigenetic investigations across diverse realms of biological research (Kaya-Okur et al., 2019).

B. Aim of the study

Cancer is a leading cause of death in the Western world, second only to cardiovascular diseases. Lung cancer (LC), including non-small cell lung cancer (NSCLC, which makes up 85% of LC cases, with around 480.000 new cases annually in the EU) and small cell lung cancer (SCLC, representing the remaining 15%), is the most lethal form of cancer across both men and women (European Cancer Information System). Currently, a significant number of lung cancer patients are treated with platinum-based chemotherapy, which often leads to severe side effects and limited success. The discovery of new therapeutic targets and treatments for NSCLC, and especially SCLC, is critically important in the era of precision medicine.

The homologous recombination repair (HRR) pathway is essential for protecting cells from genomic damage caused by both internal and external factors. Homologous recombination deficiency (HRD) is common in cancer due to various genetic and epigenetic alterations and is associated with increased sensitivity to platinum-based chemotherapy and the inhibition of PARP1/2 with PARP inhibitors (PARPi).

BRCA1/2 mutations are well-established as predisposing factors for tumor sensitivity to PARP inhibitors (PARPi) due to their critical role in DNA repair processes. However, it is noteworthy that over 40% of patients exhibit resistance to PARPi treatment. The primary resistance mechanisms include the restoration of homologous recombination repair, protection of DNA replication forks, reversion mutations, and epigenetic modifications. Thus, addressing these obstacles is imperative to enhance the efficacy of PARPi therapy.

This study is divided into two primary objectives: (1) the optimization of advanced chromatin profiling techniques (CUT&Tag, ATAC-seq), and (2) the assessment of cisplatin and olaparib (PARPi) response in patient-derived lung cancer cell lines. Achieving these objectives will enable the design and execution of a new series of experiments that will uncover novel resistance mechanisms to PARP inhibition and platinum-based chemotherapy and identify several candidate biomarkers for these treatments. Specifically for PARPi, these experiments will identify mechanisms beyond those associated with homologous recombination repair, thereby broadening the current understanding of PARPi resistance.

C. Materials & Methods

C.1 Bacterial transformation

We thawed 10 µL of NEB #C3013 cells, mixed them gently, and carefully pipetted them into a tube on ice. We then added 1 µL containing 1 pg-100 ng of plasmid DNA to the cell mixture and carefully flicked the tube 4-5 times to mix the cells and DNA, being careful not to vortex. We placed the mixture on ice for 30 minutes without mixing. Next, we performed a heat shock at exactly 42°C for 10 seconds, ensuring we did not mix the contents. Afterward, we placed the tube on ice for 5 minutes without mixing. We then pipetted 950 µL of room temperature SOC into the mixture. While warming the selection plates to 37°C, we spread 50 µL of each dilution onto a selection plate and incubated them overnight at 37°C.

C.2 pA-Tn5 purification

We transformed HIS-tagged pA-Tn5 plasmids (addgene, #171871) into NEB C3013 competent cells, which were plated on LB plates and incubated overnight at 37°C. The next day, we scraped some cells and started a 30 mL 2x YT-Amp culture, which was incubated at 37°C overnight. We then transferred the 30 mL culture to 300 mL of fresh medium and grew it at 37°C for 1-2 hours, until the culture reached an OD600

of about 0.6. Afterward, we chilled the culture to 10°C on ice and added IPTG to a final concentration of 0.25 mM. We continued to grow the culture at 18°C for approximately 4 hours, until the OD600 reached about 2.0. Next, we spun down the cells, washed them with PBS, and transferred the pellets into two 50-mL tubes. We resuspended the pellets in 12 mL of Lysis Buffer*, supplemented with 1 mM PMSF, and incubated the mixture on ice for 15 minutes. We ensured the solution was completely resuspended to achieve a homogeneous mixture. The cells were then sonicated 20 times, each cycle lasting 15 seconds on and 15 seconds off at 25% amplitude, with the probe reaching the 7.5 mL mark. We spun down the pellet twice at 2.000 g for 30 minutes at 4°C, and transferred the supernatant into new 50-mL tubes. We added 40 μL of pre-washed Ni-NTA beads to the supernatants and rotated the mixture at 4°C overnight. After incubation, we washed the beads three times with Lysis Buffer and resuspended them in 30 μL of ice-cold Elution Buffer**. We rotated the suspension at 4°C for 10 minutes and carefully transferred the supernatants into a new tube. The elution step was repeated twice, and the eluates were collected into separate tubes. We then took a small sample of the eluent or beads for SDS-PAGE to check the pA-Tn5 expression (123 kDa). If necessary, we combined the eluates and measured the protein concentrations. Finally, we added an equal volume of 100% glycerol, supplemented with protease inhibitor cocktail (PIC) and 1 mM DTT, to the eluates, aliquoted the samples, and stored them at -20°C or -80°C for long-term storage.

* Lysis Buffer

50 mM Tris-HCl, pH=8

1 M NaCl

20 mM Imidazole (I202, Sigma Aldrich)

0.1% Triton X-100

1 mM PMSF (A0999, BioChemica)

** Elution Buffer

50 mM Tris-HCl, pH=8.0

1 M NaCl

125 mM Imidazole

0.1% Triton X-100

Complete PIC

C.3 Cell culture splitting

We aspirated the DMEM medium from the cell culture plates. We then washed the cells with 3 mL of phosphate-buffered saline (PBS) to remove any residual media and serum. After aspirating the PBS completely from the plates, we added 2 mL of trypsin-EDTA solution to the plate to detach the adherent cells. We incubated the plate at 37°C for 2 minutes to allow for cell detachment. Once the cells were

detached, we carefully collected the trypsinized cells by pipetting and transferred the cell suspension into a centrifuge tube. To collect any remaining cells, we washed the plate surface with 2 mL of fresh DMEM medium and added this wash to the tube containing the trypsinized cells. We gently mixed the cell suspension to ensure homogeneity. Finally, we plated 200 μL of the cell suspension into a new culture plate and added 10 mL of DMEM for a 1:20 dilution. We labeled the new plate with the appropriate cell line information, passage number, and date.

C.4 Cell freezing

We aspirated the DMEM medium from the cell culture plates and added 3 mL of sterile PBS to the plate, gently swirling to wash the cells. After removing the PBS completely, we added 2 mL of Trypsin-EDTA solution to detach the adherent cells. We incubated the plate at 37°C for 2 minutes to allow cell detachment, then aspirated the trypsinized cells into a centrifuge tube. We rinsed the plate with 2 mL of DMEM and transferred the rinse to the same centrifuge tube, mixing thoroughly to ensure complete cell collection. The cell suspension was centrifuged at 0.4 g for 4 minutes, after which we discarded the supernatant without disturbing the cell pellet. We resuspended the cell pellet in 2 mL of freezing medium (10% DMSO in DMEM) and divided the suspension evenly into 4 cryovials. Finally, we stored the cryovials at -80°C for long-term preservation.

C.5 CUT&Tag

Tn5-adapter complex formation:

We annealed each of the Mosaic end - adapter A (ME-A) and Mosaic end - adapter B (ME-B) oligonucleotides with the Mosaic end - reverse oligonucleotides by mixing them in a 1:1 ratio and incubating the mixture at 92°C for 2 minutes, followed by a slow cooling to 4°C. We then mixed 16 µL of the 100 µM equimolar mixture of pre-annealed ME-A and ME-B oligonucleotides with 100 µL of the 5.5 µM protein A - Tn5 fusion protein. The mixture was incubated on a rotating platform for 1 hour at room temperature, and afterward, we stored it at -20°C.

Harvest and bind cells to beads:

We dissociated the cells using Trypsin and counted them. After determining the required number of cells, we centrifuged the sample at 600 g for 3 minutes. We discarded the supernatant and resuspended the pellets in Wash Buffer before centrifuging again at 600 g for 3 minutes. We then discarded the supernatant once more and resuspended the cells in 1 mL of Wash Buffer (for up to 2.5 million cells, scaling up as needed for larger cell numbers) in a 1.5 mL tube, gently. Next, we added pre-washed ConA-coated magnet beads (10 µL beads for up to 0.25 million cells, scaling up for higher cell numbers), which we had prepared while waiting for the centrifugation. We mixed the sample well and allowed it to rotate at room temperature

for 10-20 minutes. Finally, we placed the tubes on a magnet stand to discard all the supernatant.

Bind 1st antibody:

We resuspended the beads in 100 μL of ice-cold Antibody Buffer (fresh-made, which we prepared while waiting for the beads incubation) gently. Then, we added the appropriate amount of primary antibody (at a dilution of 1:100-1:200, depending on the antibody concentration). After mixing well, we placed the mixture on a nutator at 4℃ overnight.

Pre-bind 2nd antibody to Tn5:

We mixed the 2nd antibody, Tn5, and 50% glycerol up to a total volume of 8 μL per sample. For anti-rabbit, we added 1 μL per sample, and for anti-mouse, we used 2 μL per sample. The amount of Tn5 was determined based on the enzyme activity, typically using 1-2 μL per sample. Afterward, we incubated the mixture at room temperature for 1 hour.

Bind 2nd antibody and pA-Tn5 adaptor complex:

We made fresh Dig-wash buffer (1 mL per sample) and Dig-300 buffer (1 mL per sample per wash, performing 3-4 washes in total). The Dig-wash buffer was prepared by adding digitonin to the wash buffer, with the concentration depending on the cell

type. For the Dig-300 buffer, we mixed the wash buffer with 5M NaCl (300 µL per 10 mL) and digitonin at 0.01%. Afterward, we placed the tubes on a magnet stand to discard all the supernatant. The beads were washed once with 1 mL of Dig-wash buffer. Once we removed all the supernatant, we resuspended the beads in 100 µL of Dig-300 buffer. We then added 8 µL of pre-mixed second antibody and Tn5 to each sample. The samples were placed on a nutator for 1 hour at room temperature, ensuring the beads were well-resuspended.

Tagmentation:

We placed the tubes on a magnet stand to discard all the supernatant. Then, we washed the beads with 1 mL of Dig-300 buffer three times, inverting the tubes 10 times for each wash and allowing the beads to remain in the Dig-300 buffer for 3 minutes per wash. Afterward, we resuspended the beads in 250 µL of Tagmentation buffer and incubated them at 37℃ on a Thermo-mixer at 850 rpm for 1 hour. We added 10 µL of 0.5 M EDTA, 3 µL of 10% SDS (final concentration of 0.1%), and 2.5 µL of 20 mg/mL proteinase K (Macherey-Nagel) to each sample at room temperature, mixing well to stop the tagmentation. Finally, we incubated the samples at 50℃ for 1 hour or at 37℃ overnight on the Thermo-mixer to digest.

DNA extraction:

We added 300 µL of phenol-chloroform-isoamyl alcohol (PCI) to the beads/supernatant mixture and vortexed at full speed for 10 seconds. We then

centrifuged the mixture at 16.000 g at room temperature for 3 minutes. Next, we added 300 µL of chloroform, inverted the tube 10 times, and centrifuged again at 16.000 g at room temperature for 3 minutes. After this, we carefully transferred the aqueous layer to a fresh tube containing 750 µL of 100% ethanol, pipetting up and down to mix well. We chilled the mixture on ice and centrifuged it at 16.000 g at 4°C for 15 minutes. After centrifugation, we carefully poured off the liquid and drained the tube on a paper towel. We then added 1 mL of 100% ethanol to the tube and centrifuged at 16.000 g at 4°C for 1 minute. Again, we carefully poured off the liquid and drained the tube on a paper towel, allowing it to air dry until no liquid remained. Finally, we dissolved the pellet in 23 µL of low EDTA TE buffer containing 1/400 RNase A and incubated it at 37°C for 10 minutes, after which the CUT&Tag DNA was in solution.

PCR amplification and purification:

We mixed 21 µL of DNA, 2 µL of universal primer (10 µM), and 2 µL of unique index primer (10 µM) in a PCR tube. We then added 25 µL of NEBNext (New England Biolabs) 2× PCR mix. Following this, we ran the PCR program with the lid heat on:

- 72℃, 5 min
- 98℃, 30 sec
- 98℃, 10 sec
- 63℃, 10 sec

13 cycles

- 72℃, 1 min
- 10℃, hold

We added 1.1 volume (55 µL/sample) of pre-warmed NucleoMag beads (Macherey-Nagel, cat#744970) to the samples after the PCR was completed. We mixed the samples well and incubated them at room temperature for at least 10 minutes. Then, we placed the samples on the magnetic rack and waited for about 5 minutes for the beads to sediment. We carefully discarded the supernatant and washed the beads twice with 80% ethanol. After the last ethanol wash, we air-dried the tubes for 5 minutes. We then resuspended the beads in 25 µL of 10 mM Tris-HCl pH 8 and incubated them at room temperature for 5 minutes. Once again, we placed the tubes on the magnetic rack and waited for about 5 minutes for the beads to sediment. Finally, we carefully transferred the supernatant (20 µL) to a fresh tube, and the library was now in the solution, ready for quantification and sequencing.

Buffers and reagents (prepared fresh every time):

5% w/v Digitonin (Sigma-Aldrich, cat#D141):

We dissolved 5 mg in 100 µL of DMSO by mixing the solution using a vortex, and we prepared it freshly each time it was used.

10 mL Binding Buffer (storage at 4℃ for 6 months):

HEPES•KOH, pH=7.9, 20 mM, 200 µL of 1 M

KCl 10 mM, 100 µL of 1 M

$CaCl_2$ 1 mM, 10 µL of 1 M

MnCl2 1 mM, 10 µL of 1 M (J63150.AD, Thermo Scientific Chemicals)

50 mL Wash Buffer (fresh, less than 1 week):

HEPES•NaOH, pH=7.5, 20 mM, 1 mL of 1 M

NaCl 150 mM, 1.5 mL of 5 M

Spermidine 0.5 mM, 12.5 µL of 2 M

Protease inhibitor cocktail: 1 tablet /50 MI (mini 1 tablet of 10 mL)

Dig-Wash Buffer (fresh):

We added 5% Digitonin to the Wash Buffer, making the final concentration 1X-0.05%.

Antibody Buffer (fresh):

We added 4 µL of 0.5 M EDTA, 3.3 µL of 30% BSA, and Digitonin (at the required concentration) to 1 mL of Dig-Wash Buffer.

10 mL Dig-300 buffer:

We prepared it by combining the wash buffer with 300 µL of 5M NaCl and adding 0.01% digitonin.

Tagmentation buffer:

We mixed 5 mL of Dig-300 buffer with 50 µL of 1 M $MgCl_2$ to achieve a final concentration of 10 mM $MgCl_2$.

C.6 Finding the optimal concentration of cells

We prepared a 1 mL suspension of the cell culture and took 15 µL of this suspension, mixing it 1:1 with Trypan Blue. We then placed 10 µL of the mixture onto a Neubauer slide and counted the live cells. To calculate the number of cells in 1 mL, we multiplied the counted number by $2*10^4$. Next, we calculated the volume of the initial suspension containing 400.000 cells and added DMEM to achieve a new suspension of 400.000 cells in 2 mL, aiming for a starting concentration of 20.000 cells/100 µL. In a 96-well plate, we filled the peripheral wells with PBS to maintain optimal humidity. We added 200 µL of the second suspension to the three consecutive wells in the first row and placed 100 µL of DMEM into the wells directly below. From each of the three wells in the first row, we took 100 µL and diluted it by adding this volume to the wells directly below, which already contained 100 µL of DMEM. We repeated this process down the rows until we reached the final row of wells, then

discarded the last 100 μL of the suspension, preparing serial dilutions of cells starting from 20.000 cells/100 μL. Over the following days, we observed the plate under the microscope and marked the date when the wells in a row were 100% covered by cells. Finally, we determined the optimal starting concentration of cells to ensure the wells reached full coverage by day 5.

C.7 Treatments and CCK-8 viability assay

We filled the peripheral wells of the 96-well plate with PBS to maintain optimal humidity levels. We then filled the wells in triplicate with 100 μL of cell suspension at the previously calculated optimal concentration, starting from the first row and moving downstream to the last row. We filled six wells per row for each cell line and allowed them to settle for one day. In the first three wells of the first row, we added 100 μL of 20 μM cisplatin, and in the next three wells, we added 100 μL of 100 μM olaparib. In subsequent rows, we performed serial dilutions of cisplatin and olaparib treatments. On the final day (Day 5), we measured cell viability using the CCK-8 assay.

CCK-8 assay:

We pre-incubated the plate in a humidified incubator at 37 °C with 5% CO2. Afterward, we added 10 μL of the CCK-8 solution to each well of the plate, ensuring no bubbles were introduced, as they could interfere with the O.D. reading. We

incubated the plate for 1 hour in the incubator and then measured the absorbance at 450 nm using a microplate reader.

C.8 Omni-ATAC

Buffers and Reagents**:**

ATAC-Resuspension Buffer (RSB) (1.1 mL/reaction):

We prepared a 50 mL solution by adding 500 μL of 1M Tris-HCl (pH 7.4), 100 μL of 5M NaCl, and 150 μL of 1M MgCl2 to a container. Then, we added 49.25 mL of distilled water to bring the final volume to 50 mL.

ATAC-Lysis buffer (50 μL/reaction):

We prepared it by combining ATAC-RSB with 0.1% NP40, 0.1% Tween-20, and 0.01% Digitonin.

ATAC-Wash buffer (1 mL/reaction):

We prepared the ATAC-Wash buffer by combining 1 mL of ATAC-RSB with 0.1% Tween-20, ensuring that neither NP40 nor Digitonin were included in the mixture.

Transposition buffer (50 µL/reaction):

First, we mixed 2x TD buffer, which contained 20 mM Tris HCl (pH 7.5), 10 mM MgCl2, and 20% Dimethyl Formamide. We then added 1.25 µL of transposase, achieving a final concentration of 50 nM, followed by 16.5 µL of PBS. To this, we included 0.5 µL of 1% Digitonin and 0.5 µL of 10% Tween-20. Finally, we topped up the volume with 5 µL of H2O.

Tn5-adapter complex formation:

As described in C.5.

Optimized Transposition Reaction:

We pelleted 25.000 viable cells at 500 rcf, 4ºC for 5 minutes in a fixed-angle centrifuge. Then, we added 50 µL of cold ATAC-Lysis Buffer and pipetted up and down three times. We incubated the mixture on ice for 3 minutes, followed by a wash with 1 mL of cold ATAC-Wash Buffer, inverting the tube three times to mix. Afterward, we pelleted the nuclei at 500 g, 4ºC, for 10 minutes. We carefully aspirated all the supernatant down to the visible pellet using two pipetting steps. Next, we resuspended the pellet in 50 µL of Transposition Buffer, pipetting up and down six times. Finally, we incubated the sample at 37ºC for 30 minutes in a thermomixer at 1000 rpm.

Pre-amplification of transposed fragments:

We cleaned up the reaction using the Zymo DNA Clean and Concentrator-5 Kit (cat# D4014). To avoid cross-contaminating post-amplification products into pre-amplification samples, we made sure to use a separate kit for pre- and post-amplification steps. If we were unable to perform the cleanup immediately after transposition, we resuspended the ATAC reaction in 250 μL (5 volumes) of DNA Binding Buffer and stored it at -20°C. The DNA remained stable for at least two weeks in this buffer at that temperature. When ready to proceed, we allowed it to warm to room temperature and mixed thoroughly before loading the sample onto the column. Next, we eluted the DNA in 21 μL of elution buffer and stored it at -20°C until we were ready to amplify. This typically resulted in approximately 20 μL of product, which we used entirely in the following PCR. We amplified for 5 cycles using NEBNext 2x MasterMix. Each reaction contained 2.5 μL of 25 μM i5 primer, 2.5 μL of 25 μM i7 primer, 25 μL of 2x NEBNext master mix, and 20 μL of the transposed/cleaned-up sample. The thermocycler conditions were set as follows: 72ºC for 5 minutes, 98ºC for 30 seconds, followed by 5 cycles of [98ºC for 10 seconds, 63ºC for 30 seconds, 72ºC for 1 minute], and then held at 4ºC. After completing the amplification, we removed the tubes from the thermocycler and stored them on ice before proceeding immediately with the next steps.

qPCR amplification to determine additional cycles:

We used 5 μL (10%) of the pre-amplified mixture to run a 15 μL qPCR in order to determine the number of additional cycles needed. For this, we added 3.76 μL of

sterile water, 0.5 μL of 25 μM i5 primer, 0.5 μL of 25 μM i7 primer, 0.24 μL of 25x SYBR Gold (in DMSO), 5 μL of 2x NEBNext master mix, and 5 μL of the pre-amplified sample. The cycling conditions we used were 98ºC for 30 seconds, followed by 20 cycles of 98ºC for 10 seconds, 63ºC for 30 seconds, and 72ºC for 1 minute. After amplification, we manually assessed the amplification profiles to determine the required number of additional cycles for further amplification.

Final amplification and cleanup:

We used the remainder of the pre-amplified DNA and ran the required number of additional cycles. We placed the pre-amplified tubes, now containing 45 μL, back into the thermocycler without adding any more reagents. Afterward, we purified the final PCR reaction using a Zymo DNA Clean and Concentrator-5 Kit (cat# D4014) and eluted the DNA in 20 μL of H2O.

D. Results

D.1 In-house Tn5 production

To reduce costs and gain greater control over the quality of reagents used in our epigenetic assays, we aimed to produce the pA-Tn5 transposase enzyme in-house. Tn5 is essential for preparing sequencing libraries in protocols such as CUT&Tag and ATAC-seq, where it facilitates the insertion of sequencing adapters into accessible regions of the genome. Commercially available Tn5 is often expensive, and producing it ourselves was expected to improve cost-efficiency while ensuring a consistent supply tailored to our experimental needs.

To achieve this, we expressed the pA-Tn5 enzyme in *Escherichia coli* C3013, a high-efficiency strain optimized for protein expression. This strain, known as T7 Express lysY/Iq, minimizes basal expression of T7 RNA polymerase through the lysY gene and other regulatory elements, enhancing protein stability and yield. The pA-His6-Tn5 plasmid was used, which encodes the Tn5 transposase enzyme fused with an N-terminal His6-tag for efficient purification via nickel affinity. Following transformation of the plasmid into *E. coli* C3013, expression of Tn5 was induced through IPTG, and the protein was purified as described in the methods section. Figure 6 shows a Coomassie Blue-stained gel, with arrows indicating the bands corresponding to pA-Tn5, confirming the successful production of the enzyme.

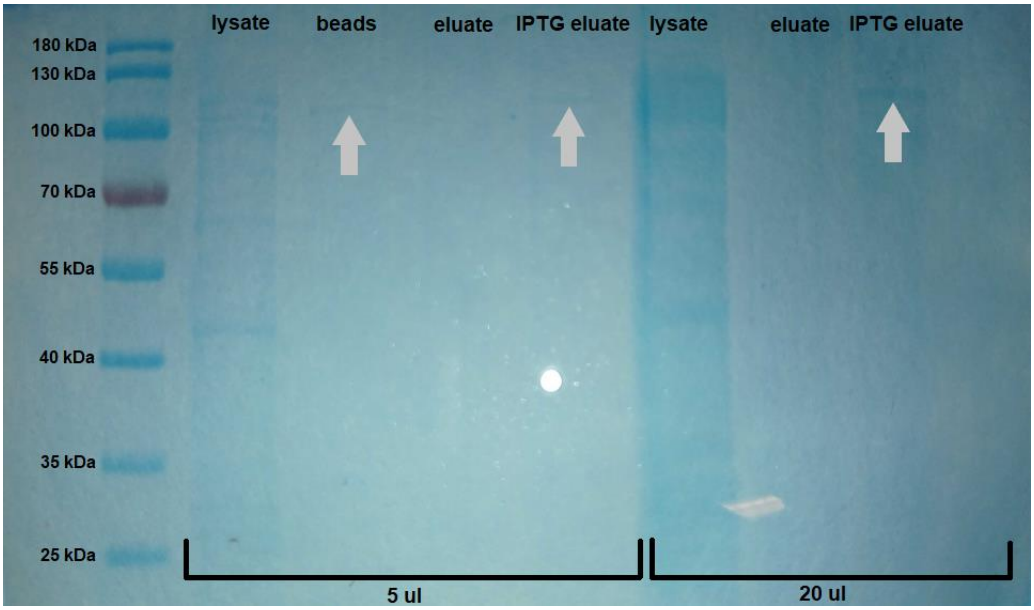

Figure 6. Confirmation of Tn5 protein expression and purification. The gel image shows the result of SDS-PAGE analysis of protein samples obtained after Tn5 expression and nickel affinity purification. A distinct band at 123 kDa corresponds to the expected size of the His6-tagged Tn5 transposase, confirming successful production. Lysate (without His6-tag purification), beads (remaining protein on Ni-NTA beads after elution), eluate (no IPTG induction), IPTG eluate (after IPTG induction).

D.2 CUT&Tag optimization

CUT&Tag optimization was conducted on a non-small cell lung cancer (NSCLC) cell line. This cell line was derived from a patient-derived xenograft (PDX), which was established from a tumor sample by members of the Klinakis lab. Use of such cancer models ensures clinical relevance. For the CUT&Tag protocol, we utilized two batches of pA-Tn5 that we produced in-house as well as pA-Tn5 enzyme from Cell Signaling Technology, as a positive control.

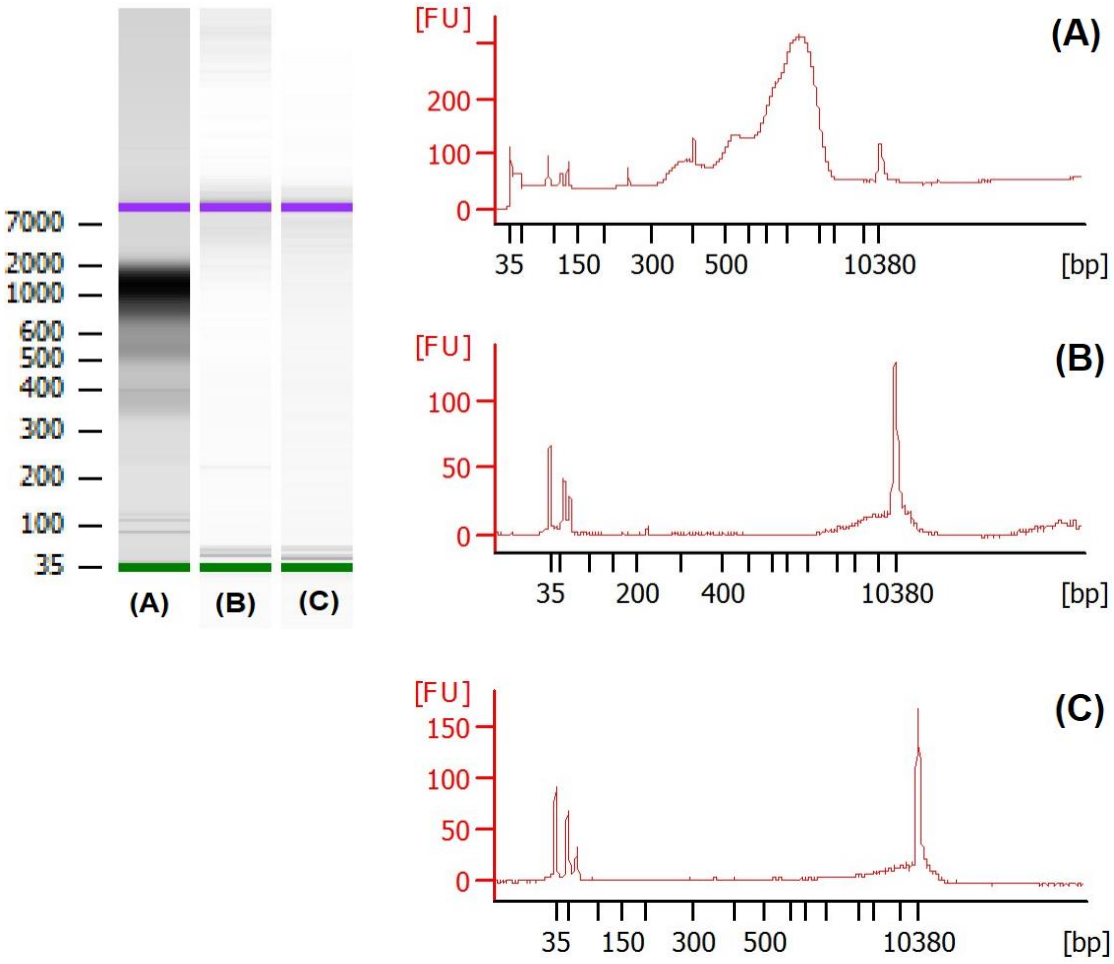

Figure 7. Agilent Bioanalyzer analysis of the CUT&Tag procedure in collaboration with the Genome Center of BRFAA. (A) commercial pA-Tn5, (B) 1st in-house batch pA-Tn5, (C) 2nd in-house batch pA-Tn5.

The quality of the CUT&Tag libraries is assessed by bioanalyzer analysis, which shows the distribution and integrity of the tagged DNA fragments following the CUT&Tag procedure. The x-axis shows the fragment size (in base pairs) and the y-axis indicates the fluorescence intensity. This analysis confirms the successful cleavage and size distribution of the DNA fragments, which are indicative of the efficiency and specificity of the CUT&Tag technique. Presence of peaks at multiples

of approximately 146 bp, which is the size of DNA wrapped around nucleosomes, suggest successful tagmentation at nucleosome-free DNA regions, while the absence of unwanted fragments confirms high purity in the assay. Sample A, obtained with the commercial pA-Tn5 enzyme, shows clear peaks at multiples of 146 bp, indicating successful tagmentation of the DNA regions (Figure 7, A). However, samples B and C, generated using batches from the in-house pA-Tn5 enzyme, display no discernible pattern and show low-quality signal, suggesting that the in-house enzyme did not function properly (Figure 7, B & C). This discrepancy emphasizes the importance of enzyme quality in the CUT&Tag protocol, as improper tagmentation can lead to poor fragment coverage and reduced assay efficiency. The commercial Tn5 enzyme likely ensured optimal tagmentation, facilitating proper sequencing and reliable data interpretation. In contrast, the lack of specific fragmentation patterns in samples B and C highlights the need for troubleshooting and optimization of the in-house enzyme preparation, possibly addressing issues such as enzyme activity, storage conditions, or contamination. Future experiments will require a careful evaluation of the in-house enzyme to improve reproducibility and data quality.

D.3 omni-ATAC optimization

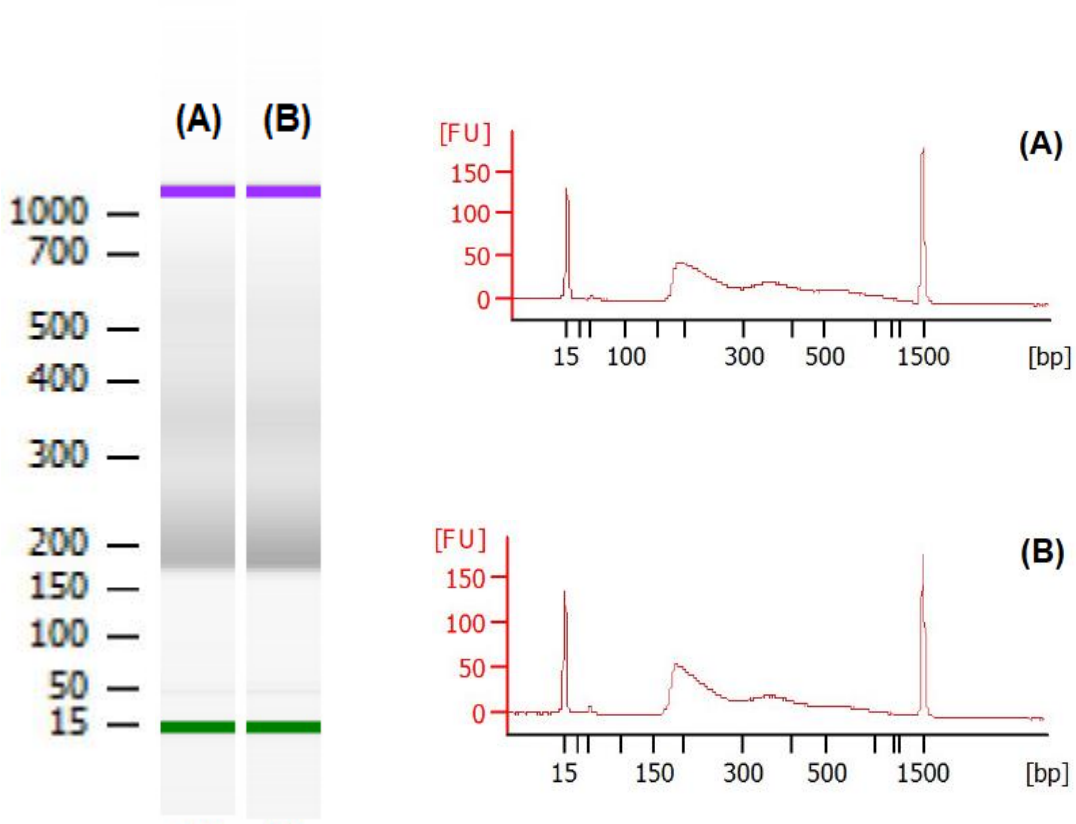

Figure 8. Agilent Bioanalyzer analysis of the omni-ATAC procedure in collaboration with the Genome Center of BRFAA. (A) Sample 1, 3.5 µL enzyme, (B) Sample 2, 5 µL enzyme.

To assess genome-wide chromatin accessibility we chose to test the efficiency of the omni-ATAC protocol in our patient-derived NSCLC cell line. We utilized a commercial Tn5 enzyme (Recombinant Tn5 Transposase protein, 10 µg, 81286, Active Motif), prepared the required buffers and reagents and executed the protocol as described in the methods section. We assessed the quality of the resulting libraries using the Agilent Bioanalyzer, in collaboration with the Genome Center of BRFAA (Figure 8). The x-axis shows the fragment size (in base pairs) and the y-axis indicates

the fluorescence intensity. The Omni-ATAC analysis reveals a discernible pattern, indicating successful tagmentation, but the overall data quality is suboptimal as indicated by the presence of high background signal. As a result, there is a need for further optimization by adjusting the number of cells.

D.4 Determining the optimal seeding density for cancer cell lines

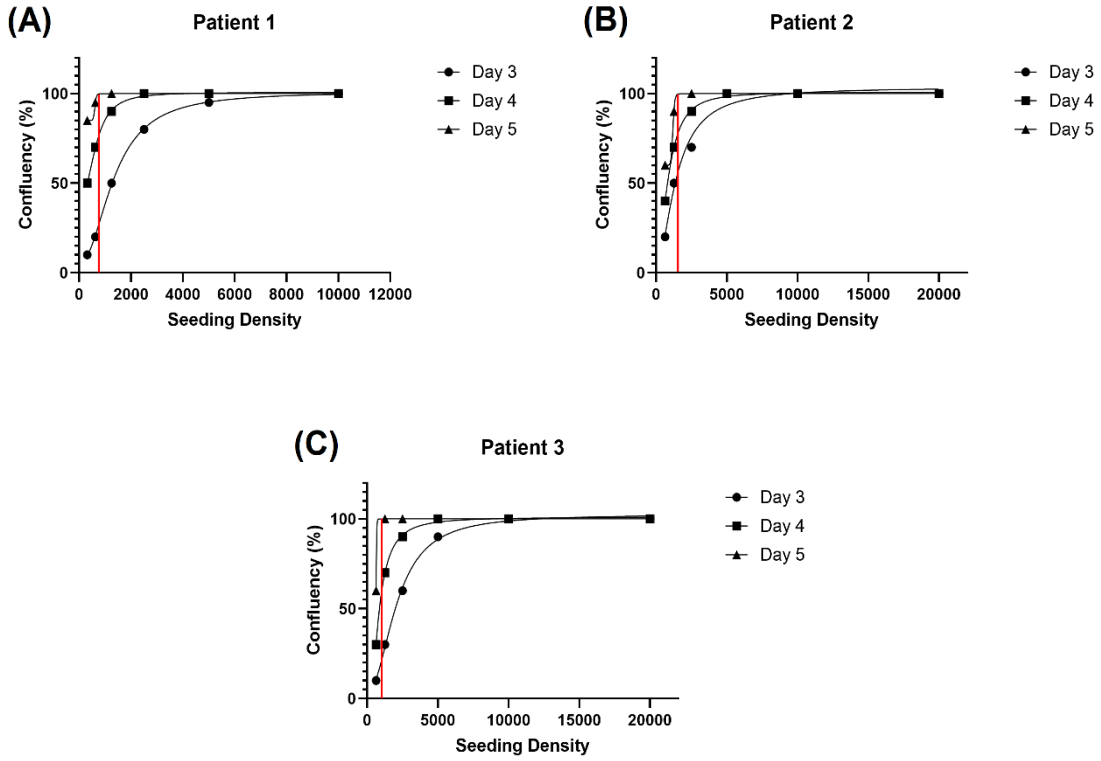

Figure 9. Graphs illustrating the daily progression of confluency levels of cells from patient 1 (A), patient 2 (B) and patient 3 (C). Red line indicates 1500 cells.

Only negligible differences were observed in the cell number required to achieve confluency by day 5 across the cell lines (Figure 9). Therefore, we selected a seeding density of 1500 cells for all cell lines, as indicated by the red line in the graphs.

D.5 Olaparib and cisplatin treatments followed by CCK-8 viability assay

To assess the sensitivity of NSCLC cell lines to PARP inhibition and platinum chemotherapy we performed a series of *in vitro* viability experiments. Three cancer cell lines, each derived from a different patient, were treated with olaparib and cisplatin (Figures 10,11,12). Of these, two cell lines (patient 2 and patient 3) were identified as homologous recombination deficiency (HRD)-positive based on their Genomic Scar Score (GSS) determined using the AmoyDx kit*, whereas the cell line derived from patient 1 was classified as HRD-negative, by other members of the Klinakis laboratory. Each graph below illustrates the effects of a specific treatment (olaparib, cisplatin) on a distinct cell line derived from the patient identified in the graph's title. The experiments were performed in triplicates or quadruplicates to ensure reliability and reproducibility.

*The AmoyDx HRD Kit uses next-generation sequencing (NGS) to detect genomic alterations linked to homologous recombination deficiency (HRD), a condition where cells struggle to repair double-strand DNA breaks. It identifies *BRCA1/2* mutations and other biomarkers associated with HRD, including loss of heterozygosity (LOH), telomeric allelic imbalance (TAI), and large-scale state transitions (LST).

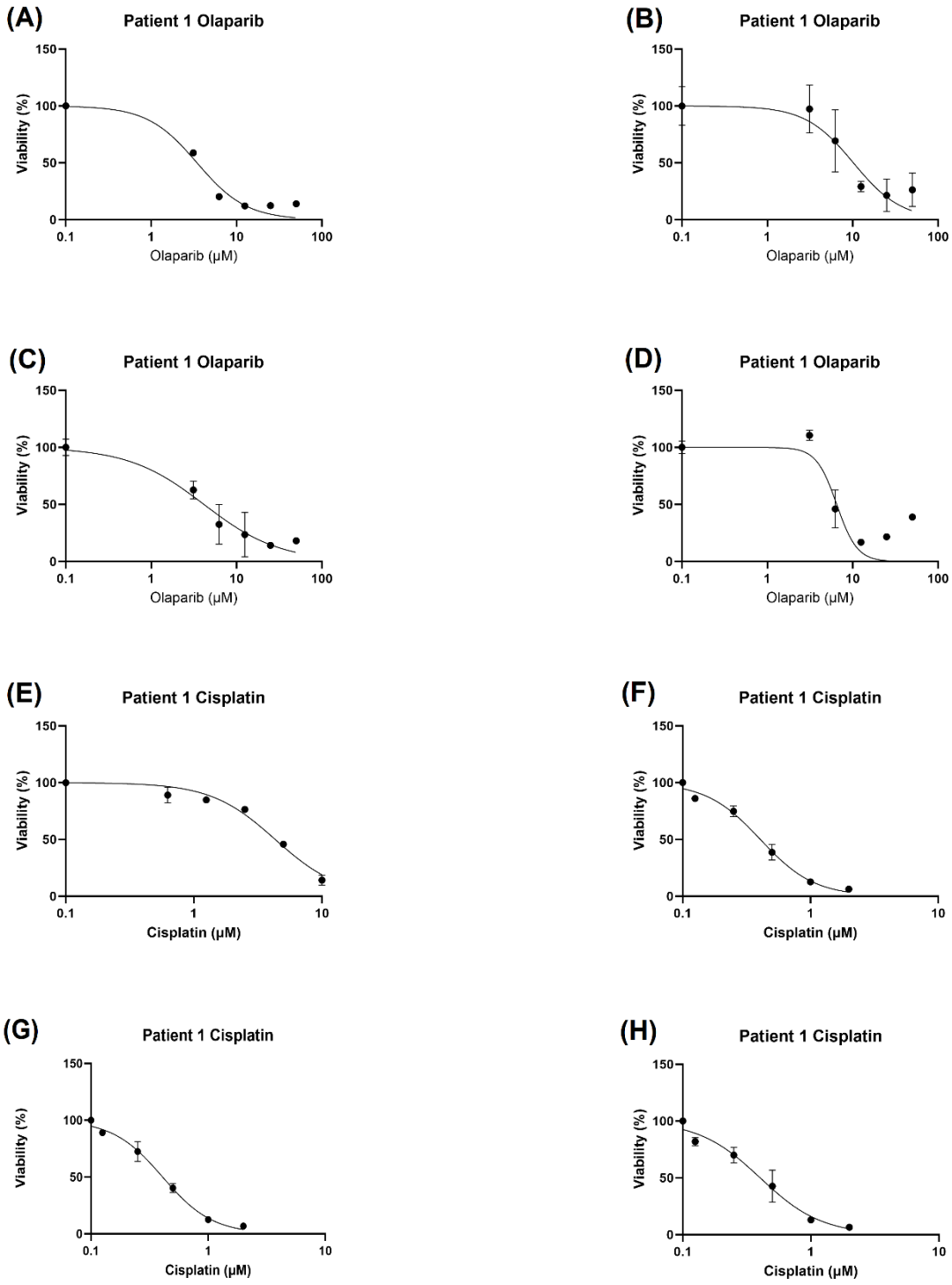

Figure 10. Graphs showing the viability (%) of cancer cells derived from patient 1 following treatment with different concentrations of olaparib (A-D) and cisplatin (E-H).

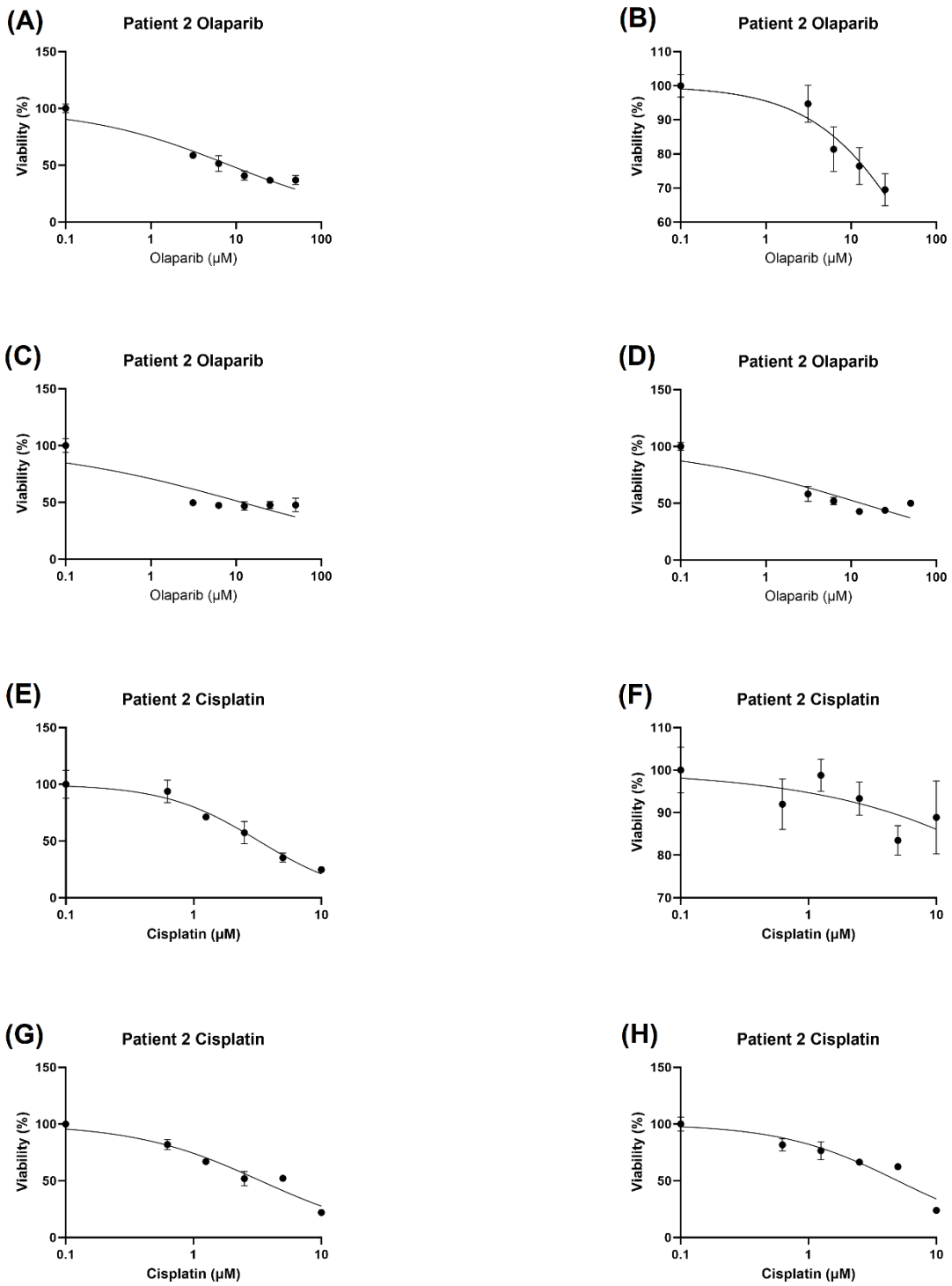

Figure 11. Graphs showing the viability (%) of cancer cells derived from patient 2 following treatment with different concentrations of olaparib (A-D) and cisplatin (E-H).

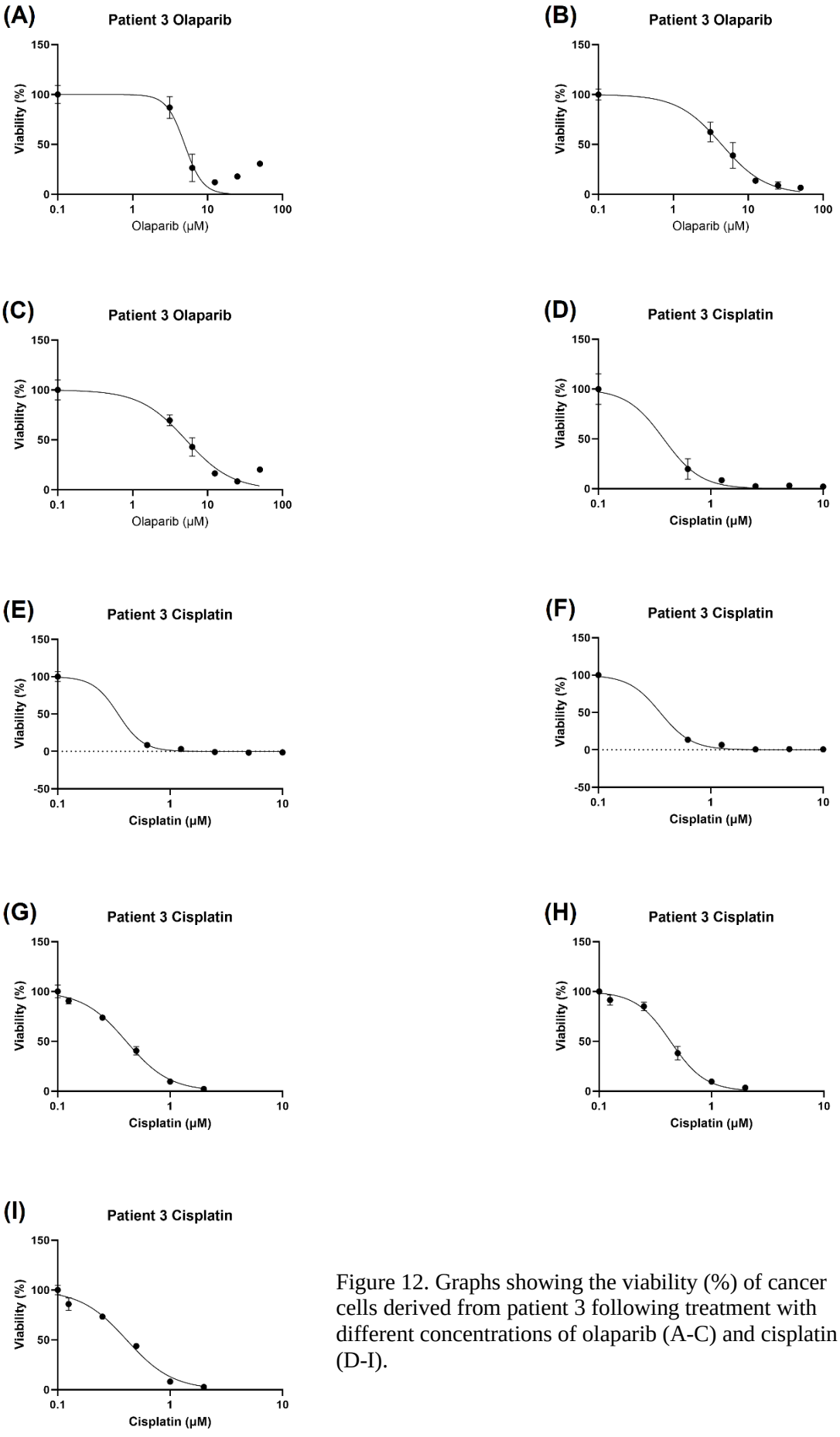

Figure 12. Graphs showing the viability (%) of cancer cells derived from patient 3 following treatment with different concentrations of olaparib (A-C) and cisplatin (D-I).

From the viability-concentration curves, we calculated the IC50 values for olaparib and cisplatin for each cancer cell line. Some experiments were excluded from the analysis due to low reproducibility and outlier measurements (Figure 10B, E, Figure 11B, F, Figure 12E, F). The variability observed (e.g., Figure 12E, F) is likely attributed to the change in the cisplatin stock, as the new stock showed a more pronounced effect on cell viability. As a result, we adjusted the experimental conditions by using a lower starting concentration of cisplatin (Figure 10F-H, Figure 12G-I). Graph generation and statistical analysis were performed using GraphPad Prism.

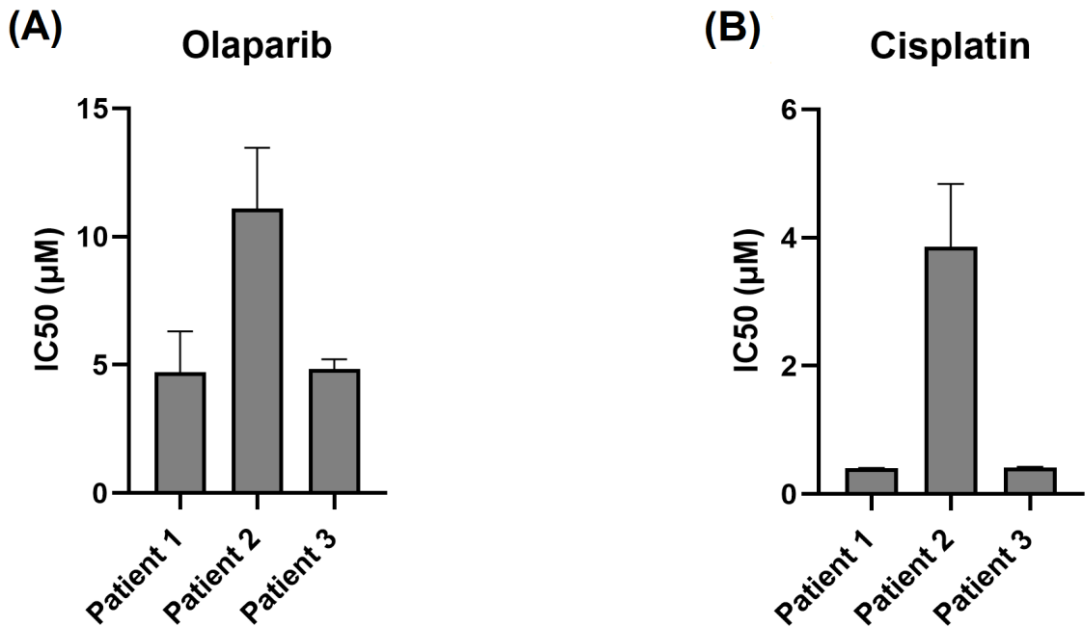

Figure 13. Column graphs displaying the IC50 values of olaparib (A) and cisplatin (B) on three distinct cancer cell lines derived from patients 1, 2, and 3. Each bar represents the IC50 concentration (in micromolar units) required to reduce cell viability by 50%.

E. Discussion

The experiments conducted thus far provide a solid foundation for future experiments and studies aiming to understand epigenomic reprogramming in the context of cancer treatment. Key methodological optimizations, such as the CUT&Tag and Omni-ATAC assays, were successfully achieved, ensuring high-quality data in subsequent stages of the study. The determination of optimal seeding densities for three cancer cell lines, including two HR-deficient lines, was essential to ensure uniform growth conditions, minimizing variability in viability assays.

IC50 values for both drugs were calculated based on the CCK-8 viability assay, highlighting differences in drug response between the cell lines. However, during the cisplatin treatments, we encountered a critical experimental variable: the depletion of the initial cisplatin stock and the subsequent use of a new stock. Despite using the same starting concentration (10 μM) and performing four serial dilutions, the new stock displayed a more pronounced cytotoxic effect, as evidenced by a dramatic decrease in cell viability, even at lower concentrations. This observation, likely due to differences in potency between the two cisplatin batches, necessitated the recalibration of experimental conditions, including using a lower starting concentration in follow-up experiments.

This adjustment highlights the inherent challenges in ensuring batch-to-batch consistency in chemical reagents and underscores the importance of proper chemical storage, use of aliquots and validation of each stock's potency. Despite these challenges, the recalibrated experiments produced consistent data, allowing for the

determination of IC50 values. These findings emphasize the need for careful monitoring of experimental variables, particularly when working with highly sensitive assays and treatments. By overcoming these challenges, we have established a reliable platform for studying the interplay between treatment-induced cytotoxicity and epigenetic reprogramming.

In this panel, we observe that HR-deficient cancer cell lines are not more sensitive to olaparib or cisplatin treatments compared to the HR-proficient cell line. This finding contrasts with *in vivo* experiments performed in patient-derived xenografts (PDXs) from the same patients. One possible explanation is the difference in treatment response between *in vivo* and *in vitro* conditions. Alternatively, the cell lines may not fully recapitulate the genetic and/or epigenetic characteristics of the PDXs from which they were derived, potentially due to the selection of specific clones during derivation and long-term *in vitro* culture. In any case, more cell lines are needed in order to assess statistical significance and draw conclusions.

Building on the results obtained thus far, the next phase of this study will focus on temporal epigenomic profiling following drug treatments. Cancer cell lines will be treated with IC50 concentrations of olaparib and the recalibrated cisplatin concentrations. Samples will be collected at 0 hours, 8 hours, 3 days, and 7 days to capture dynamic epigenetic changes. Comprehensive analyses will be performed using RNA-seq to identify transcriptional changes over time, ATAC-seq to assess alterations in chromatin accessibility and CUT&Tag to map histone modifications that regulate gene expression and repression. By integrating RNA-seq, ATAC-seq, and CUT&Tag data, we aim to uncover key pathways and regulatory networks involved in drug response and resistance mechanisms. Key genes and pathways identified will

undergo validation through functional studies, such as CRISPR-based knockdown or overexpression experiments, to confirm their roles in treatment resistance. Insights from these studies could reveal biomarkers for predicting therapeutic outcomes and identify novel targets for combination therapies aimed at overcoming resistance. This research holds potential for advancing personalized therapeutic strategies in oncology.

F. Bibliography

Akbari, M., & Krokan, H. E. (2008). Cytotoxicity and mutagenicity of endogenous DNA base lesions as potential cause of human aging. *Mechanisms of Ageing and Development*, *129*(7–8), 353–365. https://doi.org/10.1016/J.MAD.2008.01.007

ALLFREY, V. G., FAULKNER, R., & MIRSKY, A. E. (1964). ACETYLATION AND METHYLATION OF HISTONES AND THEIR POSSIBLE ROLE IN THE. *Proceedings of the National Academy of Sciences of the United States Of*, *51*(5), 786–794. https://doi.org/10.1073/PNAS.51.5.786/ASSET/8C54DEE7-DD18-4CC2-86A1-BD41B3751D13/ASSETS/PNAS.51.5.786.FP.PNG

Almeida, K. H., & Sobol, R. W. (2007). A unified view of base excision repair: lesion-dependent protein complexes regulated by post-translational modification. *DNA Repair*, *6*(6), 695–711. https://doi.org/10.1016/J.DNAREP.2007.01.009

Bajbouj, K., Al-ali, A., Ramakrishnan, R. K., Saber-ayad, M., & Hamid, Q. (2021). Histone Modification in NSCLC: Molecular Mechanisms and Therapeutic Targets. *International Journal of Molecular Sciences*, *22*(21). https://doi.org/10.3390/IJMS222111701

Balgkouranidou, I., Liloglou, T., & Lianidou, E. S. (2013a). Lung cancer epigenetics: emerging biomarkers. *Biomarkers in Medicine*, *7*(1), 49–58. https://doi.org/10.2217/BMM.12.111

Balgkouranidou, I., Liloglou, T., & Lianidou, E. S. (2013b). Lung cancer epigenetics: emerging biomarkers. *Biomarkers in Medicine*, *7*(1), 49–58. https://doi.org/10.2217/BMM.12.111

Bannister, A. J., & Kouzarides, T. (2011). Regulation of chromatin by histone modifications. *Cell Research 2011 21:3*, *21*(3), 381–395. https://doi.org/10.1038/cr.2011.22

Bartling, B., Hofmann, H. S., Boettger, T., Hansen, G., Burdach, S., Silber, R. E., & Simm, A. (2005). Comparative application of antibody and gene array for expression profiling in human squamous cell lung carcinoma. *Lung Cancer (Amsterdam, Netherlands)*, *49*(2), 145–154. https://doi.org/10.1016/J.LUNGCAN.2005.02.006

Belinsky, S. A., Nikula, K. J., Palmisano, W. A., Michels, R., Saccomanno, G., Gabrielson, E., Baylin, S. B., & Herman, J. G. (1998). Aberrant methylation of p16(INK4a) is an early event in lung cancer and a potential biomarker for early diagnosis. *Proceedings of the National Academy of Sciences of the United States of America*, *95*(20), 11891–11896. https://doi.org/10.1073/PNAS.95.20.11891

Bohr, V. A., Okumoto, D. S., & Hanawalt, P. C. (1986). Survival of UV-irradiated mammalian cells correlates with efficient DNA repair in an essential gene. *Proceedings of the National Academy of Sciences of the United States of America*, *83*(11), 3830–3833. https://doi.org/10.1073/PNAS.83.11.3830

Brock, M. V., Hooker, C. M., Ota-Machida, E., Han, Y., Guo, M., Ames, S., Glöckner, S., Piantadosi, S., Gabrielson, E., Pridham, G., Pelosky, K., Belinsky, S. A., Yang, S. C., Baylin, S. B., & Herman, J. G. (2008). DNA methylation markers and early recurrence

in stage I lung cancer. *The New England Journal of Medicine*, *358*(11), 1118–1128. https://doi.org/10.1056/NEJMOA0706550

Bryant, H. E., Schultz, N., Thomas, H. D., Parker, K. M., Flower, D., Lopez, E., Kyle, S., Meuth, M., Curtin, N. J., & Helleday, T. (2005). Specific killing of BRCA2-deficient tumours with inhibitors of poly(ADP-ribose) polymerase. *Nature*, *434*(7035), 913–917. https://doi.org/10.1038/NATURE03443

Brzeziańska, E., Dutkowska, A., & Antczak, A. (2013a). The significance of epigenetic alterations in lung carcinogenesis. *Molecular Biology Reports*, *40*(1), 309–325. https://doi.org/10.1007/S11033-012-2063-4

Brzeziańska, E., Dutkowska, A., & Antczak, A. (2013b). The significance of epigenetic alterations in lung carcinogenesis. *Molecular Biology Reports*, *40*(1), 309–325. https://doi.org/10.1007/S11033-012-2063-4

Burma, S., Chen, B. P. C., & Chen, D. J. (2006). Role of non-homologous end joining (NHEJ) in maintaining genomic integrity. *DNA Repair*, *5*(9–10), 1042–1048. https://doi.org/10.1016/J.DNAREP.2006.05.026

Cahill, D., Connor, B., & Carney, J. P. (2006). Mechanisms of eukaryotic DNA double strand break repair. *Frontiers in Bioscience : A Journal and Virtual Library*, *11*(2 P.1591-2006), 1958–1976. https://doi.org/10.2741/1938

Caldecott, K. W. (2007). Mammalian single-strand break repair: mechanisms and links with chromatin. *DNA Repair*, *6*(4), 443–453. https://doi.org/10.1016/J.DNAREP.2006.10.006

Caracciolo, D., Riillo, C., Di Martino, M. T., Tagliaferri, P., & Tassone, P. (2021). Alternative Non-Homologous End-Joining: Error-Prone DNA Repair as Cancer's Achilles' Heel. *Cancers*, *13*(6), 1–14. https://doi.org/10.3390/CANCERS13061392

Casamassimi, A., & Ciccodicola, A. (2019). Transcriptional Regulation: Molecules, Involved Mechanisms, and Misregulation. *International Journal of Molecular Sciences*, *20*(6). https://doi.org/10.3390/IJMS20061281

Casamassimi, A., Federico, A., Rienzo, M., Esposito, S., & Ciccodicola, A. (2017). Transcriptome Profiling in Human Diseases: New Advances and Perspectives. *International Journal of Molecular Sciences*, *18*(8). https://doi.org/10.3390/IJMS18081652

Chen, K., Zhao, B. S., & He, C. (2016). Nucleic Acid Modifications in Regulation of Gene Expression. *Cell Chemical Biology*, *23*(1), 74–85. https://doi.org/10.1016/J.CHEMBIOL.2015.11.007

Chromosomes and Chromatin - The Cell - NCBI Bookshelf. (n.d.). Retrieved February 4, 2024, from https://www.ncbi.nlm.nih.gov/books/NBK9863/#A620

Chu, G., & Chang, E. (1988). Xeroderma pigmentosum group E cells lack a nuclear factor that binds to damaged DNA. *Science (New York, N.Y.)*, *242*(4878), 564–567. https://doi.org/10.1126/SCIENCE.3175673

Cross, S. H., Charlton, J. A., Nan, X., & Bird, A. P. (1994). Purification of CpG islands using a methylated DNA binding column. *Nature Genetics*, *6*(3), 236–244. https://doi.org/10.1038/NG0394-236

Damiani, L. A., Yingling, C. M., Leng, S., Romo, P. E., Nakamura, J., & Belinsky, S. A. (2008). Carcinogen-induced gene promoter hypermethylation is mediated by DNMT1 and causal for transformation of immortalized bronchial epithelial cells. *Cancer Research*, *68*(21), 9005–9014. https://doi.org/10.1158/0008-5472.CAN-08-1276

Davies, J. O. J., Oudelaar, A. M., Higgs, D. R., & Hughes, J. R. (2017). How best to identify chromosomal interactions: a comparison of approaches. *Nature Methods*, *14*(2), 125–134. https://doi.org/10.1038/NMETH.4146

Dawicki-McKenna, J. M., Langelier, M. F., DeNizio, J. E., Riccio, A. A., Cao, C. D., Karch, K. R., McCauley, M., Steffen, J. D., Black, B. E., & Pascal, J. M. (2015). PARP-1 Activation Requires Local Unfolding of an Autoinhibitory Domain. *Molecular Cell*, *60*(5), 755–768. https://doi.org/10.1016/J.MOLCEL.2015.10.013

De Caceres, I. I., Cortes-Sempere, M., Moratilla, C., MacHado-Pinilla, R., Rodriguez-Fanjul, V., Manguán-García, C., Cejas, P., López-Ríos, F., Paz-Ares, L., De Castrocarpẽo, J., Nistal, M., Belda-Iniesta, C., & Perona, R. (2010). IGFBP-3 hypermethylation-derived deficiency mediates cisplatin resistance in non-small-cell lung cancer. *Oncogene*, *29*(11), 1681–1690. https://doi.org/10.1038/ONC.2009.454

De Jager, M., Van Noort, J., Van Gent, D. C., Dekker, C., Kanaar, R., & Wyman, C. (2001). Human Rad50/Mre11 is a flexible complex that can tether DNA ends. *Molecular Cell*, *8*(5), 1129–1135. https://doi.org/10.1016/S1097-2765(01)00381-1

Dhillon, K. K., Bajrami, I., Taniguchi, T., & Lord, C. J. (2016). Synthetic lethality: the road to novel therapies for breast cancer. *Endocrine-Related Cancer*, *23*(10), T39–T55. https://doi.org/10.1530/ERC-16-0228

Di Pierro, M., Cheng, R. R., Aiden, E. L., Wolynes, P. G., & Onuchic, J. N. (2017). De novo prediction of human chromosome structures: Epigenetic marking patterns encode genome architecture. *Proceedings of the National Academy of Sciences of the United States of America*, *114*(46), 12126–12131. https://doi.org/10.1073/PNAS.1714980114

Ehrich, M., Nelson, M. R., Stanssens, P., Zabeau, M., Liloglou, T., Xinarianos, G., Cantor, C. R., Field, J. K., & Van Den Boom, D. (2005). Quantitative high-throughput analysis of DNA methylation patterns by base-specific cleavage and mass spectrometry. *Proceedings of the National Academy of Sciences of the United States of America*, *102*(44), 15785–15790. https://doi.org/10.1073/PNAS.0507816102

El-Khamisy, S. F., Katyal, S., Patel, P., Ju, L., McKinnon, P. J., & Caldecott, K. W. (2009). Synergistic decrease of DNA single-strand break repair rates in mouse neural cells lacking both Tdp1 and aprataxin. *DNA Repair*, *8*(6), 760–766. https://doi.org/10.1016/J.DNAREP.2009.02.002

Fabbri, M., Garzon, R., Cimmino, A., Liu, Z., Zanesi, N., Callegari, E., Liu, S., Alder, H., Costinean, S., Fernandez-Cymering, C., Volinia, S., Guler, G., Morrison, C. D., Chan, K. K., Marcucci, G., Calin, G. A., Huebner, K., & Croce, C. M. (2007). MicroRNA-29 family reverts aberrant methylation in lung cancer by targeting DNA methyltransferases 3A and 3B. *Proceedings of the National Academy of Sciences of the United States of America*, *104*(40), 15805–15810. https://doi.org/10.1073/PNAS.0707628104

Farmer, H., McCabe, H., Lord, C. J., Tutt, A. H. J., Johnson, D. A., Richardson, T. B., Santarosa, M., Dillon, K. J., Hickson, I., Knights, C., Martin, N. M. B., Jackson, S. P., Smith, G. C. M., & Ashworth, A. (2005). Targeting the DNA repair defect in BRCA

mutant cells as a therapeutic strategy. *Nature*, *434*(7035), 917–921. https://doi.org/10.1038/NATURE03445

Forde, P. M., Brahmer, J. R., & Kelly, R. J. (2014). New strategies in lung cancer: epigenetic therapy for non-small cell lung cancer. *Clinical Cancer Research : An Official Journal of the American Association for Cancer Research*, *20*(9), 2244–2248. https://doi.org/10.1158/1078-0432.CCR-13-2088

Fousteri, M., & Mullenders, L. H. F. (2008). Transcription-coupled nucleotide excision repair in mammalian cells: molecular mechanisms and biological effects. *Cell Research*, *18*(1), 73–84. https://doi.org/10.1038/CR.2008.6

Fousteri, M., Vermeulen, W., van Zeeland, A. A., & Mullenders, L. H. F. (2006). RETRACTED: Cockayne syndrome A and B proteins differentially regulate recruitment of chromatin remodeling and repair factors to stalled RNA polymerase II in vivo. *Molecular Cell*, *23*(4), 471–482. https://doi.org/10.1016/J.MOLCEL.2006.06.029

Frommer, M., McDonald, L. E., Millar, D. S., Collis, C. M., Watt, F., Grigg, G. W., Molloy, P. L., & Paul, C. L. (1992). A genomic sequencing protocol that yields a positive display of 5-methylcytosine residues in individual DNA strands. *Proceedings of the National Academy of Sciences of the United States of America*, *89*(5), 1827. https://doi.org/10.1073/PNAS.89.5.1827

Gade, P., & Kalvakolanu, D. V. (2012). Chromatin Immunoprecipitation Assay as a Tool for Analyzing Transcription Factor Activity. *Methods in Molecular Biology (Clifton, N.J.)*, *809*, 85. https://doi.org/10.1007/978-1-61779-376-9_6

Gates, L. A., Foulds, C. E., & O'Malley, B. W. (2017). Histone Marks in the "Driver's Seat": Functional Roles in Steering the Transcription Cycle. *Trends in Biochemical Sciences*, *42*(12), 977–989. https://doi.org/10.1016/J.TIBS.2017.10.004

Giglia-Mari, G., Zotter, A., & Vermeulen, W. (2011). DNA Damage Response. *Cold Spring Harbor Perspectives in Biology*, *3*(1), 1–19. https://doi.org/10.1101/CSHPERSPECT.A000745

Gillet, L. C. J., & Schärer, O. D. (2006). Molecular mechanisms of mammalian global genome nucleotide excision repair. *Chemical Reviews*, *106*(2), 253–276. https://doi.org/10.1021/CR040483F

Goll, M. G., & Bestor, T. H. (2005). Eukaryotic cytosine methyltransferases. *Annual Review of Biochemistry*, *74*, 481–514. https://doi.org/10.1146/ANNUREV.BIOCHEM.74.010904.153721

Gueven, N., Becherel, O. J., Kijas, A. W., Chen, P., Howe, O., Rudolpg, J. H., Gatti, R., Date, H., Onodera, O., Taucher-Scholz, G., & Lavin, M. F. (2004). Aprataxin, a novel protein that protects against genotoxic stress. *Human Molecular Genetics*, *13*(10), 1081–1093. https://doi.org/10.1093/HMG/DDH122

Hanawalt, P. C. (1994). Transcription-coupled repair and human disease. *Science (New York, N.Y.)*, *266*(5193), 1957–1958. https://doi.org/10.1126/SCIENCE.7801121

He, L., & Hannon, G. J. (2004). MicroRNAs: small RNAs with a big role in gene regulation. *Nature Reviews. Genetics*, *5*(7), 522–531. https://doi.org/10.1038/NRG1379

Hegde, M. L., Hazra, T. K., & Mitra, S. (2008). Early steps in the DNA base excision/single-strand interruption repair pathway in mammalian cells. *Cell Research*, *18*(1), 27–47. https://doi.org/10.1038/CR.2008.8

Heintzman, N. D., Stuart, R. K., Hon, G., Fu, Y., Ching, C. W., Hawkins, R. D., Barrera, L. O., Van Calcar, S., Qu, C., Ching, K. A., Wang, W., Weng, Z., Green, R. D., Crawford, G. E., & Ren, B. (2007). Distinct and predictive chromatin signatures of transcriptional promoters and enhancers in the human genome. *Nature Genetics 2007 39:3*, *39*(3), 311–318. https://doi.org/10.1038/ng1966

Helleday, T., Lo, J., van Gent, D. C., & Engelward, B. P. (2007). DNA double-strand break repair: from mechanistic understanding to cancer treatment. *DNA Repair*, *6*(7), 923–935. https://doi.org/10.1016/J.DNAREP.2007.02.006

Heller, G., Weinzierl, M., Noll, C., Babinsky, V., Ziegler, B., Altenberger, C., Minichsdorfer, C., Lang, G., Döme, B., End-Pfützenreuter, A., Arns, B. M., Grin, Y., Klepetko, W., Zielinski, C. C., & Zöchbauer-Müller, S. (2012). Genome-wide miRNA expression profiling identifies miR-9-3 and miR-193a as targets for DNA methylation in non-small cell lung cancers. *Clinical Cancer Research : An Official Journal of the American Association for Cancer Research*, *18*(6), 1619–1629. https://doi.org/10.1158/1078-0432.CCR-11-2450

Hirsch, F. R., Scagliotti, G. V., Mulshine, J. L., Kwon, R., Curran, W. J., Wu, Y. L., & Paz-Ares, L. (2017). Lung cancer: current therapies and new targeted treatments. *Lancet (London, England)*, *389*(10066), 299–311. https://doi.org/10.1016/S0140-6736(16)30958-8

Hoeijmakers, J. H. J. (1993). Nucleotide excision repair. II: From yeast to mammals. *Trends in Genetics : TIG*, *9*(6), 211–217. https://doi.org/10.1016/0168-9525(93)90121-W

Imre, G., Gekeler, V., Leja, A., Beckers, T., & Boehm, M. (2006). Histone deacetylase inhibitors suppress the inducibility of nuclear factor-kappaB by tumor necrosis factor-alpha receptor-1 down-regulation. *Cancer Research*, *66*(10), 5409–5418. https://doi.org/10.1158/0008-5472.CAN-05-4225

John, A. O., & Ramnath, N. (2023). Neoadjuvant Versus Adjuvant Systemic Therapy for Early-Stage Non-Small Cell Lung Cancer: The Changing Landscape Due to Immunotherapy. *The Oncologist*, *28*(9), 752–764. https://doi.org/10.1093/ONCOLO/OYAD125

Jones, P. A., & Baylin, S. B. (2002a). The fundamental role of epigenetic events in cancer. *Nature Reviews. Genetics*, *3*(6), 415–428. https://doi.org/10.1038/NRG816

Jones, P. A., & Baylin, S. B. (2002b). The fundamental role of epigenetic events in cancer. *Nature Reviews. Genetics*, *3*(6), 415–428. https://doi.org/10.1038/NRG816

Jones, P. A., & Takai, D. (2001). The role of DNA methylation in mammalian epigenetics. *Science (New York, N.Y.)*, *293*(5532), 1068–1070. https://doi.org/10.1126/SCIENCE.1063852

Kaya-Okur, H. S., Wu, S. J., Codomo, C. A., Pledger, E. S., Bryson, T. D., Henikoff, J. G., Ahmad, K., & Henikoff, S. (2019). CUT&Tag for efficient epigenomic profiling of small samples and single cells. *Nature Communications*, *10*(1). https://doi.org/10.1038/S41467-019-09982-5

Keeney, S., Eker, A. P. M., Brody, T., Vermeulen, W., Bootsma, D., Hoeijmaker, J. H. J., & Linn, S. (1994). Correction of the DNA repair defect in xeroderma pigmentosum group E by injection of a DNA damage-binding protein. *Proceedings of the National Academy of Sciences of the United States of America*, *91*(9), 4053–4056. https://doi.org/10.1073/PNAS.91.9.4053

Kim, H., Kwon, Y. M., Kim, J. S., Han, J., Shim, Y. M., Park, J., & Kim, D. H. (2006). Elevated mRNA levels of DNA methyltransferase-1 as an independent prognostic factor in primary nonsmall cell lung cancer. *Cancer*, *107*(5), 1042–1049. https://doi.org/10.1002/CNCR.22087

King, M. C. (2014). "The race" to clone BRCA1. *Science (New York, N.Y.)*, *343*(6178), 1462–1465. https://doi.org/10.1126/SCIENCE.1251900

KORCH, C., & HAGBLOM, P. (1986). In-vivo-modified gonococcal plasmid pJD1. A model system for analysis of restriction enzyme sensitivity to DNA modifications. *European Journal of Biochemistry*, *161*(3), 519–524. https://doi.org/10.1111/J.1432-1033.1986.TB10473.X

Koschmann, C., Nunez, F. J., Mendez, F., Brosnan-Cashman, J. A., Meeker, A. K., Lowenstein, P. R., & Castro, M. G. (2017). Mutated Chromatin Regulatory Factors as Tumor Drivers in Cancer. *Cancer Research*, *77*(2), 227. https://doi.org/10.1158/0008-5472.CAN-16-2301

Lee, T. I., & Young, R. A. (2013). Transcriptional regulation and its misregulation in disease. *Cell*, *152*(6), 1237–1251. https://doi.org/10.1016/J.CELL.2013.02.014

Li, J., Li, W. X., Bai, C., & Song, Y. (2017). Particulate matter-induced epigenetic changes and lung cancer. *The Clinical Respiratory Journal*, *11*(5), 539–546. https://doi.org/10.1111/CRJ.12389

Li, Y. (2021). Modern epigenetics methods in biological research. *Methods*, *187*, 104–113. https://doi.org/10.1016/J.YMETH.2020.06.022

Liloglou, T., Bediaga, N. G., Brown, B. R. B., Field, J. K., & Davies, M. P. A. (2014). Epigenetic biomarkers in lung cancer. *Cancer Letters*, *342*(2), 200–212. https://doi.org/10.1016/J.CANLET.2012.04.018

Limbo, O., Chahwan, C., Yamada, Y., de Bruin, R. A. M., Wittenberg, C., & Russell, P. (2007). Ctp1 is a cell-cycle-regulated protein that functions with Mre11 complex to control double-strand break repair by homologous recombination. *Molecular Cell*, *28*(1), 134–146. https://doi.org/10.1016/J.MOLCEL.2007.09.009

Lindahl, T. (1993). Instability and decay of the primary structure of DNA. *Nature*, *362*(6422), 709–715. https://doi.org/10.1038/362709A0

Liu, M., & Schatz, D. G. (2009). Balancing AID and DNA repair during somatic hypermutation. *Trends in Immunology*, *30*(4), 173–181. https://doi.org/10.1016/J.IT.2009.01.007

Lord, C. J., & Ashworth, A. (2017). PARP Inhibitors: The First Synthetic Lethal Targeted Therapy. *Science (New York, N.Y.)*, *355*(6330), 1152. https://doi.org/10.1126/SCIENCE.AAM7344

Lu, C., Ward, P. S., Kapoor, G. S., Rohle, D., Turcan, S., Abdel-Wahab, O., Edwards, C. R., Khanin, R., Figueroa, M. E., Melnick, A., Wellen, K. E., Oĝrourke, D. M., Berger, S. L.,

Chan, T. A., Levine, R. L., Mellinghoff, I. K., & Thompson, C. B. (2012). IDH mutation impairs histone demethylation and results in a block to cell differentiation. *Nature*, *483*(7390), 474–478. https://doi.org/10.1038/NATURE10860

Masutani, C., Sugasawa, K., Yanagisawa, J., Sonoyama, T., Ui, M., Enomoto, T., Takio, K., Tanaka, K., Van Der Spek, P. J., Bootsma, D., Hoeijmakers, J. H. J., & Hanaoka, F. (1994). Purification and cloning of a nucleotide excision repair complex involving the xeroderma pigmentosum group C protein and a human homologue of yeast RAD23. *The EMBO Journal*, *13*(8), 1831–1843. https://doi.org/10.1002/J.1460-2075.1994.TB06452.X

Melnikov, A. A., Gartenhaus, R. B., Levenson, A. S., Motchoulskaia, N. A., & Levenson, V. V. (2005). MSRE-PCR for analysis of gene-specific DNA methylation. *Nucleic Acids Research*, *33*(10), 1–7. https://doi.org/10.1093/NAR/GNI092

Mezger, A., Klemm, S., Mann, I., Brower, K., Mir, A., Bostick, M., Farmer, A., Fordyce, P., Linnarsson, S., & Greenleaf, W. (2018). High-throughput chromatin accessibility profiling at single-cell resolution. *Nature Communications*, *9*(1). https://doi.org/10.1038/S41467-018-05887-X

Miki, Y., Swensen, J., Shattuck-Eidens, D., Futreal, P. A., Harshman, K., Tavtigian, S., Liu, Q., Cochran, C., Bennett, L. M., Ding, W., Bell, R., Rosenthal, J., Hussey, C., Tran, T., McClure, M., Frye, C., Hattier, T., Phelps, R., Haugen-Strano, A., … Skolnick, M. H. (1994). A strong candidate for the breast and ovarian cancer susceptibility gene BRCA1. *Science (New York, N.Y.)*, *266*(5182), 66–71. https://doi.org/10.1126/SCIENCE.7545954

Mitchell, J. R., Hoeijmakers, J. H. J., & Niedernhofer, L. J. (2003). Divide and conquer: Nucleotide excision repair battles cancer and ageing. *Current Opinion in Cell Biology*, *15*(2), 232–240. https://doi.org/10.1016/S0955-0674(03)00018-8

Miyanaga, A., Gemma, A., Noro, R., Kataoka, K., Matsuda, K., Nara, M., Okano, T., Seike, M., Yoshimura, A., Kawakami, A., Uesaka, H., Nakae, H., & Kudoh, S. (2008). Antitumor activity of histone deacetylase inhibitors in non-small cell lung cancer cells: development of a molecular predictive model. *Molecular Cancer Therapeutics*, *7*(7), 1923–1930. https://doi.org/10.1158/1535-7163.MCT-07-2140

Moser, J., Kool, H., Giakzidis, I., Caldecott, K., Mullenders, L. H. F., & Fousteri, M. I. (2007). RETRACTED: Sealing of chromosomal DNA nicks during nucleotide excision repair requires XRCC1 and DNA ligase III alpha in a cell-cycle-specific manner. *Molecular Cell*, *27*(2), 311–323. https://doi.org/10.1016/J.MOLCEL.2007.06.014

Moynahan, M. E., & Jasin, M. (2010). Mitotic homologous recombination maintains genomic stability and suppresses tumorigenesis. *Nature Reviews. Molecular Cell Biology*, *11*(3), 196–207. https://doi.org/10.1038/NRM2851

Moynahan, M. E., Pierce, A. J., & Jasin, M. (2001). BRCA2 is required for homology-directed repair of chromosomal breaks. *Molecular Cell*, *7*(2), 263–272. https://doi.org/10.1016/S1097-2765(01)00174-5

Murai, J., Huang, S. Y. N., Das, B. B., Renaud, A., Zhang, Y., Doroshow, J. H., Ji, J., Takeda, S., & Pommier, Y. (2012). Trapping of PARP1 and PARP2 by Clinical PARP Inhibitors. *Cancer Research*, *72*(21), 5588–5599. https://doi.org/10.1158/0008-5472.CAN-12-2753

Murai, J., Huang, S. Y. N., Renaud, A., Zhang, Y., Ji, J., Takeda, S., Morris, J., Teicher, B., Doroshow, J. H., & Pommier, Y. (2014). Stereospecific PARP trapping by BMN 673 and comparison with olaparib and rucaparib. *Molecular Cancer Therapeutics*, *13*(2), 433–443. https://doi.org/10.1158/1535-7163.MCT-13-0803

Musselman, C. A., Lalonde, M. E., Côté, J., & Kutateladze, T. G. (2012). Perceiving the epigenetic landscape through histone readers. *Nature Structural & Molecular Biology 2012 19:12*, *19*(12), 1218–1227. https://doi.org/10.1038/nsmb.2436

O'Donovan, A., Davies, A. A., Moggs, J. G., West, S. C., & Wood, R. D. (1994). XPG endonuclease makes the 3' incision in human DNA nucleotide excision repair. *Nature*, *371*(6496), 432–435. https://doi.org/10.1038/371432A0

Ogi, T., Limsirichaikul, S., Overmeer, R. M., Volker, M., Takenaka, K., Cloney, R., Nakazawa, Y., Niimi, A., Miki, Y., Jaspers, N. G., Mullenders, L. H. F., Yamashita, S., Fousteri, M. I., & Lehmann, A. R. (2010). Three DNA polymerases, recruited by different mechanisms, carry out NER repair synthesis in human cells. *Molecular Cell*, *37*(5), 714–727. https://doi.org/10.1016/J.MOLCEL.2010.02.009

Özdağ, H., Teschendorff, A. E., Ahmed, A. A., Hyland, S. J., Blenkiron, C., Bobrow, L., Veerakumarasivam, A., Burtt, G., Subkhankulova, T., Arends, M. J., Collins, V. P., Bowtell, D., Kouzarides, T., Brenton, J. D., & Caldas, C. (2006). Differential expression of selected histone modifier genes in human solid cancers. *BMC Genomics*, *7*. https://doi.org/10.1186/1471-2164-7-90

Ozsolak, F., Poling, L. L., Wang, Z., Liu, H., Liu, X. S., Roeder, R. G., Zhang, X., Song, J. S., & Fisher, D. E. (2008a). Chromatin structure analyses identify miRNA promoters. *Genes & Development*, *22*(22), 3172–3183. https://doi.org/10.1101/GAD.1706508

Ozsolak, F., Poling, L. L., Wang, Z., Liu, H., Liu, X. S., Roeder, R. G., Zhang, X., Song, J. S., & Fisher, D. E. (2008b). Chromatin structure analyses identify miRNA promoters. *Genes & Development*, *22*(22), 3172–3183. https://doi.org/10.1101/GAD.1706508

Pettitt, S. J., Rehman, F. L., Bajrami, I., Brough, R., Wallberg, F., Kozarewa, I., Fenwick, K., Assiotis, I., Chen, L., Campbell, J., Lord, C. J., & Ashworth, A. (2013). A genetic screen using the PiggyBac transposon in haploid cells identifies Parp1 as a mediator of olaparib toxicity. *PloS One*, *8*(4). https://doi.org/10.1371/JOURNAL.PONE.0061520

Picelli, S., Björklund, Å. K., Reinius, B., Sagasser, S., Winberg, G., & Sandberg, R. (2014). Tn5 transposase and tagmentation procedures for massively scaled sequencing projects. *Genome Research*, *24*(12), 2033–2040. https://doi.org/10.1101/GR.177881.114

Policastro, R. A., & Zentner, G. E. (2018). Enzymatic methods for genome-wide profiling of protein binding sites. *Briefings in Functional Genomics*, *17*(2), 138–145. https://doi.org/10.1093/BFGP/ELX030

Pommier, Y., O'Connor, M. J., & De Bono, J. (2016). Laying a trap to kill cancer cells: PARP inhibitors and their mechanisms of action. *Science Translational Medicine*, *8*(362). https://doi.org/10.1126/SCITRANSLMED.AAF9246

Qi, Y., & Zhang, B. (2019). Predicting three-dimensional genome organization with chromatin states. *PLoS Computational Biology*, *15*(6). https://doi.org/10.1371/JOURNAL.PCBI.1007024

Ramalingam, S. S., Owonikoko, T. K., & Khuri, F. R. (2011). Lung cancer: New biological insights and recent therapeutic advances. *CA: A Cancer Journal for Clinicians*, *61*(2), 91–112. https://doi.org/10.3322/CAAC.20102

Rauch, T., & Pfeifer, G. P. (2005). Methylated-CpG island recovery assay: a new technique for the rapid detection of methylated-CpG islands in cancer. *Laboratory Investigation; a Journal of Technical Methods and Pathology*, *85*(9), 1172–1180. https://doi.org/10.1038/LABINVEST.3700311

Reznikoff, W. S. (2003). Tn5 as a model for understanding DNA transposition. *Molecular Microbiology*, *47*(5), 1199–1206. https://doi.org/10.1046/J.1365-2958.2003.03382.X

Salazar, F., Molina, M. A., Sanchez-Ronco, M., Moran, T., Ramirez, J. L., Sanchez, J. M., Stahel, R., Garrido, P., Cobo, M., Isla, D., Bertran-Alamillo, J., Massuti, B., Cardenal, F., Manegold, C., Lianes, P., Trigo, J. M., Sanchez, J. J., Taron, M., & Rosell, R. (2011). First-line therapy and methylation status of CHFR in serum influence outcome to chemotherapy versus EGFR tyrosine kinase inhibitors as second-line therapy in stage IV non-small-cell lung cancer patients. *Lung Cancer (Amsterdam, Netherlands)*, *72*(1), 84–91. https://doi.org/10.1016/J.LUNGCAN.2010.07.008

Sartori, A. A., Lukas, C., Coates, J., Mistrik, M., Fu, S., Bartek, J., Baer, R., Lukas, J., & Jackson, S. P. (2007). Human CtIP promotes DNA end resection. *Nature*, *450*(7169), 509–514. https://doi.org/10.1038/NATURE06337

Sasaki, H., Moriyama, S., Nakashima, Y., Kobayashi, Y., Kiriyama, M., Fukai, I., Yamakawa, Y., & Fujii, Y. (2004). Histone deacetylase 1 mRNA expression in lung cancer. *Lung Cancer*, *46*(2), 171–178. https://doi.org/10.1016/j.lungcan.2004.03.021

Satoh, M. S., & Lindahl, T. (1992). Role of poly(ADP-ribose) formation in DNA repair. *Nature*, *356*(6367), 356–358. https://doi.org/10.1038/356356A0

Schadt, E. E., Turner, S., & Kasarskis, A. (2010). A window into third-generation sequencing. *Human Molecular Genetics*, *19*(R2). https://doi.org/10.1093/HMG/DDQ416

Schiano, C., Casamassimi, A., Vietri, M. T., Rienzo, M., & Napoli, C. (2014). The roles of mediator complex in cardiovascular diseases. *Biochimica et Biophysica Acta*, *1839*(6), 444–451. https://doi.org/10.1016/J.BBAGRM.2014.04.012

Schmid, M., Durussel, T., & Laemmli, U. K. (2004). ChIC and ChEC; genomic mapping of chromatin proteins. *Molecular Cell*, *16*(1), 147–157. https://doi.org/10.1016/J.MOLCEL.2004.09.007

Schwartzentruber, J., Korshunov, A., Liu, X. Y., Jones, D. T. W., Pfaff, E., Jacob, K., Sturm, D., Fontebasso, A. M., Quang, D. A. K., Tönjes, M., Hovestadt, V., Albrecht, S., Kool, M., Nantel, A., Konermann, C., Lindroth, A., Jäger, N., Rausch, T., Ryzhova, M., … Jabado, N. (2012). Driver mutations in histone H3.3 and chromatin remodelling genes in paediatric glioblastoma. *Nature*, *482*(7384), 226–231. https://doi.org/10.1038/NATURE10833

Seligson, D. B., Horvath, S., McBrian, M. A., Mah, V., Yu, H., Tze, S., Wang, Q., Chia, D., Goodglick, L., & Kurdistani, S. K. (2009). Global levels of histone modifications predict prognosis in different cancers. *The American Journal of Pathology*, *174*(5), 1619–1628. https://doi.org/10.2353/AJPATH.2009.080874

Shackelford, R. E., Kaufmann, W. K., & Paules, R. S. (1999). Cell cycle control, checkpoint mechanisms, and genotoxic stress. *Environmental Health Perspectives*, *107 Suppl 1*(Suppl 1), 5–24. https://doi.org/10.1289/EHP.99107S15

Shames, D. S., Girard, L., Gao, B., Sato, M., Lewis, C. M., Shivapurkar, N., Jiang, A., Perou, C. M., Kim, Y. H., Pollack, J. R., Fong, K. M., Lam, C. L., Wong, M., Shyr, Y., Nanda, R., Olopade, O. I., Gerald, W., Euhus, D. M., Shay, J. W., … Minna, J. D. (2006a). A genome-wide screen for promoter methylation in lung cancer identifies novel methylation markers for multiple malignancies. *PLoS Medicine*, *3*(12), 2244–2263. https://doi.org/10.1371/JOURNAL.PMED.0030486

Shames, D. S., Girard, L., Gao, B., Sato, M., Lewis, C. M., Shivapurkar, N., Jiang, A., Perou, C. M., Kim, Y. H., Pollack, J. R., Fong, K. M., Lam, C. L., Wong, M., Shyr, Y., Nanda, R., Olopade, O. I., Gerald, W., Euhus, D. M., Shay, J. W., … Minna, J. D. (2006b). A genome-wide screen for promoter methylation in lung cancer identifies novel methylation markers for multiple malignancies. *PLoS Medicine*, *3*(12), 2244–2263. https://doi.org/10.1371/JOURNAL.PMED.0030486

Shames, D. S., Girard, L., Gao, B., Sato, M., Lewis, C. M., Shivapurkar, N., Jiang, A., Perou, C. M., Kim, Y. H., Pollack, J. R., Fong, K. M., Lam, C. L., Wong, M., Shyr, Y., Nanda, R., Olopade, O. I., Gerald, W., Euhus, D. M., Shay, J. W., … Minna, J. D. (2006c). A genome-wide screen for promoter methylation in lung cancer identifies novel methylation markers for multiple malignancies. *PLoS Medicine*, *3*(12), 2244–2263. https://doi.org/10.1371/JOURNAL.PMED.0030486

Shen, H., & Laird, P. W. (2013). Interplay between the cancer genome and epigenome. *Cell*, *153*(1), 38–55. https://doi.org/10.1016/J.CELL.2013.03.008

Sierra, F., Lichtler, A., Marashi, F., Rickles, R., Van Dyke, T., Clark, S., Wells, J., Stein, G., & Stein, J. (1982). Organization of human histone genes. *Proceedings of the National Academy of Sciences*, *79*(6), 1795–1799. https://doi.org/10.1073/PNAS.79.6.1795

Sijbers, A. M., De Laat, W. L., Ariza, R. R., Biggerstaff, M., Wei, Y. F., Moggs, J. G., Carter, K. C., Shell, B. K., Evans, E., De Jong, M. C., Rademakers, S., De Rooij, J., Jaspers, N. G. J., Hoeijmakers, J. H. J., & Wood, R. D. (1996). Xeroderma pigmentosum group F caused by a defect in a structure-specific DNA repair endonuclease. *Cell*, *86*(5), 811–822. https://doi.org/10.1016/S0092-8674(00)80155-5

Sinclair, D. A., & Oberdoerffer, P. (2009). The ageing epigenome: damaged beyond repair? *Ageing Research Reviews*, *8*(3), 189–198. https://doi.org/10.1016/J.ARR.2009.04.004

Skene, P. J., Henikoff, J. G., & Henikoff, S. (2018). Targeted in situ genome-wide profiling with high efficiency for low cell numbers. *Nature Protocols*, *13*(5), 1006–1019. https://doi.org/10.1038/NPROT.2018.015

Skene, P. J., & Henikoff, S. (2017). An efficient targeted nuclease strategy for high-resolution mapping of DNA binding sites. *ELife*, *6*. https://doi.org/10.7554/ELIFE.21856

Sterlacci, W., Tzankov, A., Veits, L., Zelger, B., Bihl, M. P., Foerster, A., Augustin, F., Fiegl, M., & Savic, S. (2011). A comprehensive analysis of p16 expression, gene status, and promoter hypermethylation in surgically resected non-small cell lung carcinomas. *Journal of Thoracic Oncology : Official Publication of the International Association for the Study of Lung Cancer*, *6*(10), 1649–1657. https://doi.org/10.1097/JTO.0B013E3182295745

Strahl, B. D., & Allis, C. D. (2000). The language of covalent histone modifications. *Nature*, *403*(6765), 41–45. https://doi.org/10.1038/47412

Sugasawa, K., Akagi, J. ichi, Nishi, R., Iwai, S., & Hanaoka, F. (2009a). Two-step recognition of DNA damage for mammalian nucleotide excision repair: Directional binding of the XPC complex and DNA strand scanning. *Molecular Cell*, *36*(4), 642–653. https://doi.org/10.1016/J.MOLCEL.2009.09.035

Sugasawa, K., Akagi, J. ichi, Nishi, R., Iwai, S., & Hanaoka, F. (2009b). Two-step recognition of DNA damage for mammalian nucleotide excision repair: Directional binding of the XPC complex and DNA strand scanning. *Molecular Cell*, *36*(4), 642–653. https://doi.org/10.1016/J.MOLCEL.2009.09.035

Takeda, S., Nakamura, K., Taniguchi, Y., & Paull, T. T. (2007). Ctp1/CtIP and the MRN complex collaborate in the initial steps of homologous recombination. *Molecular Cell*, *28*(3), 351–352. https://doi.org/10.1016/J.MOLCEL.2007.10.016

Tan, M., Luo, H., Lee, S., Jin, F., Yang, J. S., Montellier, E., Buchou, T., Cheng, Z., Rousseaux, S., Rajagopal, N., Lu, Z., Ye, Z., Zhu, Q., Wysocka, J., Ye, Y., Khochbin, S., Ren, B., & Zhao, Y. (2011). Identification of 67 Histone Marks and Histone Lysine Crotonylation as a New Type of Histone Modification. *Cell*, *146*(6), 1016–1028. https://doi.org/10.1016/J.CELL.2011.08.008

Teytelman, L., Thurtle, D. M., Rine, J., & Van Oudenaarden, A. (2013). Highly expressed loci are vulnerable to misleading ChIP localization of multiple unrelated proteins. *Proceedings of the National Academy of Sciences of the United States of America*, *110*(46), 18602–18607. https://doi.org/10.1073/PNAS.1316064110

Thompson, N., Adams, D. J., & Ranzani, M. (2017). Synthetic lethality: emerging targets and opportunities in melanoma. *Pigment Cell and Melanoma Research*, *30*(2), 183–193. https://doi.org/10.1111/PCMR.12573

Toyota, M., Ahuja, N., Ohe-Toyota, M., Herman, J. G., Baylin, S. B., & Issa, J. P. J. (1999a). CpG island methylator phenotype in colorectal cancer. *Proceedings of the National Academy of Sciences of the United States of America*, *96*(15), 8681–8686. https://doi.org/10.1073/PNAS.96.15.8681

Toyota, M., Ahuja, N., Ohe-Toyota, M., Herman, J. G., Baylin, S. B., & Issa, J. P. J. (1999b). CpG island methylator phenotype in colorectal cancer. *Proceedings of the National Academy of Sciences of the United States of America*, *96*(15), 8681–8686. https://doi.org/10.1073/PNAS.96.15.8681

Tsao, A. S., Scagliotti, G. V., Bunn, P. A., Carbone, D. P., Warren, G. W., Bai, C., De Koning, H. J., Uraujh Yousaf-Khan, A., McWilliams, A., Tsao, M. S., Adusumilli, P. S., Rami-Porta, R., Asamura, H., Van Schil, P. E., Darling, G. E., Ramalingam, S. S., Gomez, D. R., Rosenzweig, K. E., Zimmermann, S., … Pass, H. I. (2016). Scientific Advances in Lung Cancer 2015. *Journal of Thoracic Oncology : Official Publication of the International Association for the Study of Lung Cancer*, *11*(5), 613–638. https://doi.org/10.1016/J.JTHO.2016.03.012

Tutt, A., Bertwistle, D., Valentine, J., Gabriel, A., Swift, S., Ross, G., Griffin, C., Thacker, J., & Ashworth, A. (2001). Mutation in Brca2 stimulates error-prone homology-directed repair of DNA double-strand breaks occurring between repeated sequences. *The EMBO Journal*, *20*(17), 4704–4716. https://doi.org/10.1093/EMBOJ/20.17.4704

Van Den Broeck, A., Brambilla, E., Moro-Sibilot, D., Lantuejoul, S., Brambilla, C., Eymin, B., Khochbin, S., & Gazzeri, S. (2008a). Loss of histone H4K20 trimethylation occurs in preneoplasia and influences prognosis of non-small cell lung cancer. *Clinical Cancer Research : An Official Journal of the American Association for Cancer Research*, *14*(22), 7237–7245. https://doi.org/10.1158/1078-0432.CCR-08-0869

Van Den Broeck, A., Brambilla, E., Moro-Sibilot, D., Lantuejoul, S., Brambilla, C., Eymin, B., Khochbin, S., & Gazzeri, S. (2008b). Loss of histone H4K20 trimethylation occurs in preneoplasia and influences prognosis of non-small cell lung cancer. *Clinical Cancer Research : An Official Journal of the American Association for Cancer Research*, *14*(22), 7237–7245. https://doi.org/10.1158/1078-0432.CCR-08-0869

Van Gent, D. C., & Van Der Burg, M. (2007). Non-homologous end-joining, a sticky affair. *Oncogene*, *26*(56), 7731–7740. https://doi.org/10.1038/SJ.ONC.1210871

Van Steensel, B., Delrow, J., & Henikoff, S. (2001). Chromatin profiling using targeted DNA adenine methyltransferase. *Nature Genetics*, *27*(3), 304–308. https://doi.org/10.1038/85871

Volker, M., Moné, M. J., Karmakar, P., Van Hoffen, A., Schul, W., Vermeulen, W., Hoeijmakers, J. H. J., Van Driel, R., Van Zeeland, A. A., & Mullenders, L. H. F. (2001). Sequential assembly of the nucleotide excision repair factors in vivo. *Molecular Cell*, *8*(1), 213–224. https://doi.org/10.1016/S1097-2765(01)00281-7

Wang, M., Vikis, H. G., Wang, Y., Jia, D., Wang, D., Bierut, L. J., Bailey-Wilson, J. E., Amos, C. I., Pinney, S. M., Petersen, G. M., De Andrade, M., Yang, P., Wiest, J. S., Fain, P. R., Schwartz, A. G., Gazdar, A., Minna, J., Gaba, C., Rothschild, H., … You, M. (2007). Identification of a novel tumor suppressor gene p34 on human chromosome 6q25.1. *Cancer Research*, *67*(1), 93–99. https://doi.org/10.1158/0008-5472.CAN-06-2723

Weinberg, R. A. (1995). The retinoblastoma protein and cell cycle control. *Cell*, *81*(3), 323–330. https://doi.org/10.1016/0092-8674(95)90385-2

Weterings, E., & Van Gent, D. C. (2004). The mechanism of non-homologous end-joining: A synopsis of synapsis. *DNA Repair*, *3*(11), 1425–1435. https://doi.org/10.1016/j.dnarep.2004.06.003

Wooster, R., Bignell, G., Lancaster, J., Swift, S., Seal, S., Mangion, J., Collins, N., Gregory, S., Gumbs, C., Micklem, G., Barfoot, R., Hamoudi, R., Patel, S., Rices, C., Biggs, P., Hashim, Y., Smith, A., Connor, F., Arason, A., … Stratton, M. R. (1995). Identification of the breast cancer susceptibility gene BRCA2. *Nature*, *378*(6559), 789–792. https://doi.org/10.1038/378789A0

Wyman, C., & Kanaar, R. (2006). DNA double-strand break repair: all's well that ends well. *Annual Review of Genetics*, *40*, 363–383. https://doi.org/10.1146/ANNUREV.GENET.40.110405.090451

Wyman, C., Ristic, D., & Kanaar, R. (2004). Homologous recombination-mediated double-strand break repair. *DNA Repair*, *3*(8–9), 827–833. https://doi.org/10.1016/j.dnarep.2004.03.037

Xi, S., Xu, H., Shan, J., Tao, Y., Hong, J. A., Inchauste, S., Zhang, M., Kunst, T. F., Mercedes, L., & Schrump, D. S. (2013). Cigarette smoke mediates epigenetic repression

of miR-487b during pulmonary carcinogenesis. *The Journal of Clinical Investigation*, *123*(3), 1241–1261. https://doi.org/10.1172/JCI61271

Yokoi, M., Masutani, C., Maekawa, T., Sugasawa, K., Ohkuma, Y., & Hanaoka, F. (2000). The xeroderma pigmentosum group C protein complex XPC-HR23B plays an important role in the recruitment of transcription factor IIH to damaged DNA. *The Journal of Biological Chemistry*, *275*(13), 9870–9875. https://doi.org/10.1074/JBC.275.13.9870

Yu, M., Hon, G. C., Szulwach, K. E., Song, C. X., Zhang, L., Kim, A., Li, X., Dai, Q., Shen, Y., Park, B., Min, J. H., Jin, P., Ren, B., & He, C. (2012). Base-resolution analysis of 5-hydroxymethylcytosine in the mammalian genome. *Cell*, *149*(6), 1368–1380. https://doi.org/10.1016/J.CELL.2012.04.027

Zentner, G. E., Kasinathan, S., Xin, B., Rohs, R., & Henikoff, S. (2015). ChEC-seq kinetics discriminates transcription factor binding sites by DNA sequence and shape in vivo. *Nature Communications*, *6*. https://doi.org/10.1038/NCOMMS9733

Zhang, G., Huang, H., Liu, D., Cheng, Y., Liu, X., Zhang, W., Yin, R., Zhang, D., Zhang, P., Liu, J., Li, C., Liu, B., Luo, Y., Zhu, Y., Zhang, N., He, S., He, C., Wang, H., & Chen, D. (2015). N6-methyladenine DNA modification in Drosophila. *Cell*, *161*(4), 893–906. https://doi.org/10.1016/J.CELL.2015.04.018

Zhang, Y., Wang, R., Song, H., Huang, G., Yi, J., Zheng, Y., Wang, J., & Chen, L. (2011). Methylation of multiple genes as a candidate biomarker in non-small cell lung cancer. *Cancer Letters*, *303*(1), 21–28. https://doi.org/10.1016/J.CANLET.2010.12.011

Zhao, H., Fan, Y., Ma, S., Song, X., Han, B., Cheng, Y., Huang, C., Yang, S., Liu, X., Liu, Y., Lu, S., Wang, J., Zhang, S., Zhou, C., Wang, M., & Zhang, L. (2015). Final overall survival results from a phase III, randomized, placebo-controlled, parallel-group study of gefitinib versus placebo as maintenance therapy in patients with locally advanced or metastatic non-small-cell lung cancer (INFORM; C-TONG 0804). *Journal of Thoracic Oncology : Official Publication of the International Association for the Study of Lung Cancer*, *10*(4), 655–664. https://doi.org/10.1097/JTO.0000000000000445

Zheng, G. X. Y., Terry, J. M., Belgrader, P., Ryvkin, P., Bent, Z. W., Wilson, R., Ziraldo, S. B., Wheeler, T. D., McDermott, G. P., Zhu, J., Gregory, M. T., Shuga, J., Montesclaros, L., Underwood, J. G., Masquelier, D. A., Nishimura, S. Y., Schnall-Levin, M., Wyatt, P. W., Hindson, C. M., … Bielas, J. H. (2017). Massively parallel digital transcriptional profiling of single cells. *Nature Communications*, *8*. https://doi.org/10.1038/NCOMMS14049